UNIVERSITY OF KWAZULU-NATAL

AN INVESTIGATION OF ELECTRIC-FIELD-GRADIENT-INDUCED BIREFRINGENCE IN FLUIDS

SIYABONGA SIBUSISO NTOMBELA

2014

An Investigation of Electric-field-gradient-induced Birefringence in Fluids

By

SIYABONGA SIBUSISO NTOMBELA
BSc Honours in Physics

Submitted in partial fulfilment of the requirements for the degree of
MSc
in the School of Chemistry and Physics
University of KwaZulu-Natal

PIETERMARITZBURG
November 2014

Contents

List of Figures

Declaration

This dissertation describes the work undertaken at the School of Chemistry and Physics, University of KwaZulu-Natal, Pietermaritzburg Campus under the supervision of Dr V. W. Couling between January 2012 and November 2014.

I declare that the work reported in this dissertation is my own research, unless specifically indicated to the contrary in the text. This dissertation has not been submitted in any form, for any degree or examination to any other university.

Signed: .....

On this ..... day of 2014

I hereby certify that this statement is correct

.....

Dr V. W. Couling

Supervisor

Acknowledgments

I would *firstly* like to give thanks to ***God, my Lord, my Saviour*** for giving me such a wonderful experience in my life time, to do research towards my masters in this preriod of time.

Secondly my supervisor *Dr V. W. Couling* for his excellent supervision towards my research project, his help was great, even towards financial support. He has been a real good, kind supervisor.

Thirdly the Principal Technician Mr K. Penzhorn: any modifications to the apparatus that required specialized workshop assistance, he undertook them with a willing heart; Mr Dewar from the Electronics Centre for his enormous assistance with the electronic components of the project; and Mr R. Sirvraman and Ms S. Khumalo of the Physics technical staff, for their laboratory assistance.

Fourthly my parents *Mr S. J. Ntombela and Mrs L. E. Ntombela* for assisting me in furthering my studies: it has meant a lot to me.

My surrounding friends, brethren and my Pastors for their support and encouragement.

Prof R. E. Raab for his assistance with techniques in scientific writing, which helped a great deal.

Last but not least I would like to thank the National Institute for Theoretical Physics (NITheP) for awarding me a bursary to study towards my masters in research.

Abstract

The theory of electric-field-gradient-induced birefringence (EFGIB, the Buckingham effect) is briefly reviewed, and modifications to the Buckingham-effect apparatus are described. These modifications have increased the throughput of the light reaching the photodiode detector, thereby considerably enhancing the sensitivity of the measurements. In addition, a new PID voltage controller has been built for the high-voltage power amplifier, ensuring stability to better than 0.1% over long periods of time. Room-temperature measurements of the Buckingham effect for gaseous oxygen have been undertaken, allowing for an estimation of the traceless electric quadrupole moment Θ of O_2. The quadrupole moment has been extracted from the measured data by making the assumption that the temperature-independent hyperpolarizability contribution to the EFGIB is negligible. The limitations of this assumption are discussed. The value obtained for the electric quadrupole moment of O_2 is $\Theta = (-1.033 \pm 0.027) \times 10^{-40}\,\mathrm{C\,m^2}$. The available *ab initio* quantum-computed values of Θ found for O_2 in the literature are tabulated, and are compared with our measured value. Potential future work, where a full temperature-dependent study of the EFGIB of O_2 is envisioned, is briefly described.

List of Acronyms

ACPF Averaged Coupled Pair Functional

CCSD(T) Coupled Cluster, Singles and Doubles with Triples treated approximately

CI Configuration Interaction

CME Cotton-Mouton Effect

DAC Digital-to-Analogue Converter

DAU Data-Acquisition and control Unit

EFGIB Electric-Field-Gradient-Induced Birefringence

HP Hewlett Packard

MCSCF MultiConfigurational Self-Consistent Field

NITheP National Institute for Theoretical Physics

PID Proportional-Integral-Derivative

PSD Phase-Sensitive Detector

RTD Resistance Temperature Detector

Chapter 1

Introduction and Theory

1.1 Introduction

The principal aim of this research project has been to measure the electric-field-gradient-induced birefringence (EFGIB) of molecular oxygen, and thereby to deduce the molecular electric quadrupole moment for this species.

The electric quadrupole moment is a fundamental property of a molecule. For non-dipolar molecules like oxygen, it is the leading electric moment which describes the molecule's charge-distribution and its interaction with external non-uniform electric fields [1, 2]. Like the dipole moment, the quadrupole moment can aid in providing a description of a range of physical properties including the thermodynamic, structural and spectral properties of molecules. It can also assist in the description of a range of physical phenomena ranging from intermolecular interaction effects to aspects of atmospheric chemical

physics [1, 3].

The molecular quadrupole moments of gaseous species can be measured directly via the method of EFGIB, or the Buckingham effect. This method was first proposed by Buckingham in 1959 [4], and was first demonstrated by Buckingham and Disch in 1963 [5]. Subsequently, many researchers have undertaken EFGIB experiments on dipolar as well as non-dipolar molecules. Recent review articles summarize many of these contributions [6, 7].

In this experiment, the gas sample is contained in a cell constructed from a hollow conducting cylinder, along the length of which are strung two thin wires separated by a small distance to allow for the passage of a light beam. If the cylinder is earthed and the wires are held at a high potential, a high electric field gradient and zero electric field will be established on the axis of the cylinder. The Laboratory-frame Cartesian axes are conveniently chosen such that the wires lie in the $yz-$plane, while the $z-$axis co-incides with the axis of the cylinder. The electric field gradient tensor $E_{\alpha\beta}$ in the region between the wires then has the form

$$\nabla_\alpha E_\beta \;=\; E_{\alpha\beta} \;=\; \begin{bmatrix} E_{xx} & 0 & 0 \\ 0 & E_{yy} = -E_{xx} & 0 \\ 0 & 0 & 0 \end{bmatrix}. \tag{1.1}$$

EFGIB is the anisotropy in the refractive index, $(n_x - n_y)$, that occurs when

linearly-polarized light propagates through the fluid along the $z-$direction, this direction being perpendicular to the applied electric field gradient $E_{xx} = -E_{yy}$. There are two separate phenomenological sources for this induced anisotropy: a temperature-independent term arising from the distortion of the electronic stucture by the field gradient, and a temperature dependent term arising from the partial alignment of the quadrupole moments by the electric field gradient. Ritchie and his co-workers have shown that the deduction of reliable quadrupole moments from EFGIB measurements requires the separation of these two contributions [8–11]. To achieve this one needs to take experimental measurements over as wide a temperature as practicably possible, usually from around room temperature to around two hundred degrees celsius.

Unfortunately, temperature-dependent EFGIB measurements present a considerable experimental challenge, especially for a species like oxygen, where the induced birefringence is exceptionally small. There is a great deal of background noise inherent at elevated temperatures, where thermal gradients can result in turbulence in fluids, adding substantially to the instability in the experiment. There has been a considerable effort in this project to achieve measurements of the EFGIB of O_2 above room temperature, but these attempts have proved fruitless, and will have to be further pursued in future PhD studies. What has been achieved is a comprehensive set of room-temperature measurements, which, coupled with the assumption that the electronic distortion contribution to the EFGIB is negligibly small, has allowed for an estimate of the quadrupole moment of oxygen. The associated caveats surrounding the

reliability and the interpretation of this quadrupole moment are thoroughlly discussed.

One of the prime reasons motivating the importance of obtaining an accurate and precise experimental measure of the quadrupole moment of O_2 lies in the testing of theoretical predictions. Unlike *ab initio* computations of molecular energies, which are primarily determined by the electron density closer to the nuclei, molecular quadrupole moments are rather sensitive to the distribution of charge in the outer regions of the molecule [12]. Hence, quadrupole moments become an excellent test of the wave functions used in their quantum-mechanical computation. Once theoreticians are able to compute quadrupole moments with sufficient accuracy, then their computed values of the higher multipole moments could be presumed to be more reliable. Accurate experimental measurement of these higher multipole moments is often currently intractable.

Bartolomei *et al.* have recently calculated the quadrupole moment of O_2 by making use of high-level multiconfigurational *ab initio* methods [13]. Attaining high accuracy in *ab initio* computations of these sorts of molecular properties presents a considerable challenge. Large basis sets must be used, together with the inclusion of electron correlation effects and vibrational averaging. These issues are thoroughlly elucidated in the comprehensive review article of Helgaker *et al.* [14]. Where possible, the measurement of accurate experimental values for these molecular properties can provide benchmarks

for the assessment of the higher levels of *ab initio* theory. The lack of sound experimental data for the quadrupole moment of O_2 against which to benchmark calculated data is one of the principal justifications for the present study.

1.2 The multipole expansion, and the definition of the electric quadrupole moment

The treatment of electric multipole moments presented here follows that of Buckingham [2]. A description of the interaction between two molecules can be reduced to a tractable problem by ignoring the internal motion of the electrons in a particular molecule, thereby allowing electrostatic theory to be invoked. If the two molecules are sufficiently separated, the electrostatic potential of a molecule can be expanded about an arbitrary origin close to its charges, which gives rise to a series of moments of charge. These moments can then be measured, and used to characterize the molecule.

Consider a distribution of charges q_i in a vacuum. Let these charges have displacements $\mathbf{r}_i$ from an arbitrary origin O which is situated close to, or within, the charge distribution. The electrostatic potential at a point P which has displacement $\mathbf{R}$ from O is

$$\phi(\mathbf{R}) = \frac{1}{4\pi\varepsilon_0} \sum_i \frac{q_i}{\mathbf{R} - \mathbf{r}_i}. \tag{1.2}$$

Provided that the point P lies sufficiently far away from the charge distribution, it becomes possible to utilize the binomial theorem in order to expand the denominator in the summation above, yielding

$$\phi(\mathbf{R}) = \frac{1}{4\pi\varepsilon_0}\left[\frac{1}{R}\sum_i q_i + \frac{R_\alpha}{R^3}\sum_i q_i r_{i\alpha} + \frac{3R_\alpha R_\beta - R^2\delta_{\alpha\beta}}{2R^5}\sum_i q_i r_{i\alpha} r_{i\beta} + \cdots\right]. \quad (1.3)$$

Here and in what follows, Cartesian components have been denoted by Greek subscripts, and a repeated Greek subscript implies a summation over x, y and z, while $\delta_{\alpha\beta}$ is the Kronecker delta tensor.

The various moments of the charge distribution can now be extracted, yielding:

the total charge

$$q = \sum_i q_i, \quad (1.4)$$

the electric dipole moment

$$\mu_\alpha = \sum_i q_i r_{i\alpha}, \quad (1.5)$$

and the electric quadrupole moment

$$Q_{\alpha\beta} = \sum_i q_i r_{i\alpha} r_{i\beta}. \tag{1.6}$$

$Q_{\alpha\beta}$ is known as the primitive quadrupole moment, however, an alternative definition known as the traceless quadrupole moment has come to be almost universally employed. Here,

$$\Theta_{\alpha\beta} = \frac{1}{2}(3Q_{\alpha\beta} - Q_{\gamma\gamma}\delta_{\alpha\beta}) = \frac{1}{2}\sum_i q_i(3r_{i\alpha}r_{i\beta} - r_i^2\delta_{\alpha\beta}). \tag{1.7}$$

The electrostatic potential can now be written in terms of these defined moments of charge, such that

$$\phi(\mathbf{R}) = \frac{1}{R}q + \frac{R_\alpha}{R^3}\mu_\alpha + \frac{3R_\alpha R_\beta - R^2\delta_{\alpha\beta}}{2R^5}Q_{\alpha\beta} + \cdots. \tag{1.8}$$

The successively higher multipole moments are seen to make successively smaller contributions to $\phi(\mathbf{R})$, so that the octopole, hexadecapole and higher-order moments will contribute much less to the potential of a molecule which is in possession of a permanent quadrupole moment, and so can be safely ignored.

1.3 Summary of the theory of EFGIB

The original semi-classical theory of EFGIB of Buckingham and Longuet-Higgins [15] was challenged in 1991 by Imrie and Raab [16], who derived a different ex-

pression relating the induced birefringence to the quadrupole moment and other molecular properties. They used an eigenvalue theory for the propagation of light in matter. Recent *ab initio* quantum-computational studies of the EFGIB for carbon monoxide [17], carbon dioxide and carbon disulphide [18], and nitrous oxide and carbonyl sulphide [19] were prompted in part by this controversy. More recently, this controversy was resolved through a revision of the existing theories, whereby the original Buckingham–Longuet-Higgins result was confirmed exactly [20–23].

EFGIB is the anisotropy in the refractive index $(n_x - n_y)$ experienced by light as it propagates through a gas along the $z-$axis of the laboratory Cartesian frame, being perpendicular to the applied electric field gradient $E_{xx} = -E_{yy}$. The molar field-gradient birefringence constant ${}_mQ$ has been defined in terms of macroscopic observables as [24]

$$ {}_mQ = \frac{6n(3\varepsilon_r + 2)}{5\varepsilon_r(n^2+2)^2} \lim_{E_{xx}\to 0} \left(\frac{n_x - n_y}{E_{xx}} \right) V_m, \tag{1.9} $$

where n and ε_r are the refractive index and relative permittivity of the gas in the absence of the field gradient, V_m being the molar volume of the gas.

O_2 has axial symmetry, and is a non-dipolar molecule, which leads to a simplification of the classical equation for the induced birefringence. Expressed in terms of fundamental molecular properties [15], ${}_mQ$ becomes

$$ {}_mQ = \frac{2N_A}{45\epsilon_0}\left[\frac{15}{2}\,b + \frac{\Theta\Delta\alpha}{kT}\right]. \tag{1.10} $$

The hyperpolarizability term b in this expression is a function of the frequency ω of the incident light, and is a grouping of molecular hyperpolarizabilities given by [15, 25]

$$ b = \frac{2}{15}\left(B_{\alpha\beta,\alpha\beta} - \mathscr{B}_{\alpha,\alpha\beta,\beta}\right) - \frac{2}{3\omega}\epsilon_{\alpha\beta\gamma}J'_{\alpha,\beta,\gamma}. \tag{1.11} $$

Here, $\epsilon_{\alpha\beta\gamma}$ is the Levi-Civita tensor, and the hyperpolarizabiliy tensors $B_{\alpha\beta,\alpha\beta}$, $\mathscr{B}_{\alpha,\alpha\beta,\beta}$ and $J'_{\alpha,\beta,\gamma}$ are defined elsewhere [15]. $\Delta\alpha$ is the dynamic dipole polarizability anisotropy, and Θ is the traceless quadrupole moment which was defined earlier.

The derivation of Eq. (1.10) is based upon the assumption that the rotational motion of the molecules is classical. For lighter molecules like O_2, the effects of the quantization of rotation on the alignment of the molecules in the applied field gradient need to be factored in, as shown by Buckingham and Pariseau [26]. Eq. (1.10) then becomes

$$ {}_mQ = \frac{2N_A}{45\epsilon_0}\left[\frac{15}{2}\,b' + \frac{\Theta\Delta\alpha}{kT}f(T)\right] \tag{1.12} $$

where, for an axially symmetric molecule with principal moment of inertia I,

$$ f(T) \;=\; 1 - \left(\frac{\hbar^2}{2kTI}\right) + \frac{8}{15}\left(\frac{\hbar^2}{2kTI}\right)^2 + \cdots. \tag{1.13} $$

b' differs from b by a small amount as a consequence of centrifugal distortion of the molecule. $f(T)$ is very close to 1 for all but the very lightest molecules, so that quantum corrections need not always be taken into account. For oxygen, $f(T)$ is 0.9931 at 300 K, leading to a small but non-negligible correction of 0.7%.

Bibliography

[1] A. D. Buckingham, *Permanent and induced molecular moments and long-range intermolecular forces,* Adv. Chem. Phys. **12,** 107 (1967).

[2] A. D. Buckingham, *Electric Moments of Molecules,* in *Physical Chemistry, An Advanced Treatise,* edited by H. Eyring, D. Henderson and W. Yost (Academic Press, New York, 1970), vol. 4, Chap. 8, pp. 349–386.

[3] M. Lepers, B. Bussery-Honvault, and O. Dulieu, *Long-range interactions in the ozone molecule: Spectroscopic and dynamical points of view,* J. Chem. Phys. **137,** 234305 (2012).

[4] A. D. Buckingham, *Direct method of measuring molecular quadrupole moments,* J. Chem. Phys. **30,** 1580 (1959).

[5] A. D. Buckingham and R. L. Disch, *The quadrupole moment of the carbon dioxide molecule*, Proc. R. Soc. Lond. A **273,** 275 (1963).

[6] G. L. D. Ritchie, *Field-gradient induced birefringence: a direct route to molecular quadrupole moments,* in *Optical, Electric and Magnetic Properties of Molecules*, edited by D. C. Clary and B. J. Orr (Elsevier, Amsterdam, 1997), Chap. 2, pp. 67–95.

[7] A. Rizzo and S. Coriani, *Birefringences: a challenge for both theory and experiment*, Adv. Quantum Chem. **50,** 143 (2005).

[8] J. N. Watson, Ph. D. thesis, *The measurement of field gradient induced birefringence in gases*, University of New England (1994).

[9] J. N. Watson, I. E. Craven, and G. L. D. Ritchie, *Temperature dependence of electric field-gradient induced birefringence in carbon dioxide and carbon disulfide*, Chem. Phys. Lett. **274,** 1 (1997).

[10] G. L. D. Ritchie and J. N. Watson, *Temperature dependence of electric field-gradient induced birefringence (the Buckingham effect) in C_6H_6 and C_6F_6:*

comparison of electric and magnetic properties of C_6H_6 and C_6F_6, Chem. Phys. Lett. **322,** 143 (2000).

[11] G. L. D. Ritchie, J. N. Watson, and R. I. Keir, *Temperature dependence of electric field-gradient induced birefringence (Buckingham effect) and molecular quadrupole moment of N_2. Comparison of experiment and theory*, Chem. Phys. Lett. **370,** 376 (2003).

[12] A. D. Buckingham and B. D. Utting, *Intermolecular forces*, Ann. Rev. Phys. Chem. **21,** 287 (1970).

[13] M. Bartolomei, E. Carmona-Novillo, M. I. Hernez, J. Campos-Martz, and R. Harnez-Lamoneda, *Long-Range interaction for dimers of atmospheric interest: Dispersion, induction and electrostatic contributions for O_2-O_2, N_2-N_2 and O_2-N_2*, J. Comp. Chem. **32,** 279 (2011).

[14] T. Helgaker, S. Coriani, P. Jørgensen, K. Kristensen, J. Olsen, K. Ruud, *Recent advances in wave function-based methods of molecular-property calculations*, Chem. Rev. **112,** 543 (2012).

[15] A. D. Buckhingham and H. C. Longuet-Higgins, *Quadrupole moments of dipolar molecules*, Mol. Phys. **14,** 63 (1968).

[16] D. A. Imrie and R. E. Raab, *A new molecular theory of field gradient induced birefringence used for measuring electric quadrupole-moments*, Mol. Phys. **74,** 833 (1991).

[17] A. Rizzo, S. Coriani, A. Halkier, and C. Hattig, *Ab initio study of the electric-field-gradient-induced birefringence of a polar molecule: CO*, J. Chem. Phys. **113,** 3077 (2000).

[18] S. Coriani, A. Halkier, A. Rizzo, and K. Ruud, *On the molecular electric quadrupole moment and the electric-field-gradient-induced birefringence of CO_2 and CS_2*, Chem. Phys. Lett. **326,** 269 (2000).

[19] S. Coriani, A. Halkier, D. Jonsson, J. Gauss, A. Rizzo, and O. Christiansen, *On the electric field gradient induced birefringence and electric quadrupole moment of CO, N_2O, and OCS*, J. Chem. Phys. **118,** 7329 (2003).

[20] R. E. Raab and O. L. de Lange, *Forward scattering theory of electric-field-gradient-induced birefringence*, Mol. Phys. **101,** 3467 (2003).

[21] O. L. de Lange and R. E. Raab, *Reconciliation of the forward scattering and wave theories of electric-field-gradient-induced birefringence,* Mol. Phys. **102,** 125 (2004).

[22] R. E. Raab and O. L. de Lange, *Multipole Theory in Electromagnetism* (Oxford: Clarendon, 2005).

[23] O. L. de Lange and R. E. Raab, *On the theory of the Buckingham effect*, Mol. Phys. **104,** 607 (2006).

[24] J. Vrbancich and G. L. D. Ritchie, *Quadrupole-moments of benzene, hexafluorobenzene and other non-dipolar aromatic molecules*, J. Chem. Soc., Faraday Trans. 2 **76,** 648 (1980).

[25] A. D. Buckingham, M. J. Jamieson, *Birefringence induced in spherical molecules by an electric field gradient*, Mol. Phys. **22,** 117 (1971).

[26] A. D. Buckingham, M. Pariseau, *Molecular quadrupole moments - quantum corrections to classical formula*, Trans. Faraday Soc. **62,** 1 (1966).

Chapter 2

Experimental

2.1 Introduction

The electric-field-gradient-induced birefringence apparatus that was used in this research project is similar to that of Buckingham and Disch described in their original investigation of CO_2 [1]. It is the same apparatus previously used by Couling and Chetty [2, 3], but has undergone considerable modification in this research project, principally to ensure that a much greater light intensity reaches the photodiode detector. The present EFGIB measurements of molecular oxygen were an extremely challenging undertaking, since the magnitude of the quadrupole moment is relatively small compared to the other species which have been investigated to date. Since the sensitivity of the measured signal is proportional to the square root of the light intensity reaching the detector, it is crucial that the light throughput is maximized as much as is practicably feasible. This project has seen an overall improvement of around 10

times the light throughput previously achieved by Couling and Chetty. This was realized through several modifications to the apparatus, including placing all of the optical components on one single optical rail, increasing the diameter of the central beam hole in the wire holder plates, as well as the use of a water Faraday cell rather than a Pockels glass Faraday cell (water transmitting more of the incident light). The power amplifier which supplies the quadrupole cell wires with their high voltage has also been significantly upgraded to achieve greater stability by making use of a new PID controller circuit. The measurement technique and the optical and electronic components are now discussed in considerable detail.

2.2 Measurement technique

The phase difference δ arising from the induced birefringence in the gas sample is the observable property that was measured in this experiment. The space-fixed axes of the laboratory frame $O(x, y, z)$ are fixed relative to the quadrupole cell such that the laser light propagates in the $z-$direction, which travels along the axis of a hollow earthed stainless-steel cylinder. Two thin parallel wires lie along the length of this axis, being spaced equidistant from it. These wires are held at the same potential. The $z-$direction is perpendicular to the resulting electric field gradient $E_{xx} = -E_{yy}$. The linearly-polarized light beam has its azimuth set at 45° relative to the $x-$axis after propagating through a calcite polarizing prism. Once a gas sample is admitted to the cell, and upon appli-

cation of the electric field gradient, that component of the light beam which is oscillating in the xz plane will experience a refractive index of n_x, while the component oscillating in the yz plane will experience a different refractive index of n_y. If the beam travels along a path length of l in the presence of the birefringent sample, then it will emerge with an induced phase difference of

$$\delta = \frac{2\pi l}{\lambda}\left(n_x - n_y\right). \tag{2.1}$$

The polarization state of this emergent beam will be elliptical in form, but after passage through a quarter-wave plate with its fast axis set at 45° relative to the $x-$axis, it will be converted back into a linear polarization state, but offset from the 45° azimuth by an angle (in radians) of $\frac{\delta}{2}$. δ is a particularly small angle, of the order of 75 nanoradians for the molecular oxygen samples in our present experimental arrangement. To extract such a tiny signal from the background noise, it is best to modulate δ so that the technique of phase-sensitive detection can be employed. The analyzer is initially crossed with the polarizer prism, and then the electric field gradient is applied to the gas sample, resulting in a signal arriving at the photodiode detector due to the optical retardation δ. This signal is nulled (i.e. brought to a minimum value) by means of a compensating device which is positioned in between the quadrupole cell and the analyzer. Our compensating device consisted of a Faraday cell, which serves to

rotate the plane of the linearly-polarized light emerging from the quarter-wave plate. By varying the magnitude of the ac current in the Faraday cell's solenoid coils, the plane of polarization of the light beam can be varied to rotate it back by $\frac{\delta}{2}$, hence bringing the signal at the detector back to null. Since the Faraday cell is accurately calibrated, the current required to achieve null can be related to a precisely quantifiable angle, leading to precise and accurate knowledge of $\frac{\delta}{2}$ in radians.

It is experimentally problematic to achieve a null signal using this technique, simply because the light intensity at the photodiode detector will be extremely small, so that the detected signal will be swamped by the background noise. Buckingham and Disch [1] demonstrated a way around this problem, making use of the linear method of optical detection described by Badoz [4]. Here, a deliberate static retardation is introduced into the optical path, achieved in practice by a small offset of around half a degree in the azimuth of either the quarter-wave plate or the analyzer. This results in an amplification of the optical signal by several orders of magnitude. By varying the current in the Faraday cell's solenoid, a plot can be achieved of the lock-in amplifier output versus this rms current. At first glance, it seems intuitive to assume that the null current would correspond to a zero lock-in amplifier ouput, but the strain birefringence present in the Pockels glass windows (which allow light to enter and exit the Buckingham cell) causes an offset. A thorough Jones-calculus analysis of the effects of the elements in the optical cascade on the polarization properties of the propagating beam was undertaken by Graham *et al.* [5]. This analysis

revealed that plots of the lock-in amplifier output versus Faraday cell rms current (and hence optical rotation) for analyzer offsets $+\varepsilon_1$ and $-\varepsilon_2$ will intersect at a point whose corresponding current is the null current. If the quarter-wave plate is offset instead of the analyzer, the Jones calculus revealed that any small deviations from the ideal retardance could lead to substantial errors in the null currents and hence in the deduced quadrupole moments.

Our experimental observations reported here were all obtained through an experimental procedure whereby the quarter-wave plate was fixed to an azimuth of 45°, with the analyzer being offset by small positive and negative rotations of around half a degree. This ensured that the null currents and hence null rotations were in essence free of any significant errors arising from the strain birefringence present in the entrance and exit windows of the quadrupole cell. The deduced quadrupole moments were thus also essentially free from this source of error.

2.3 Apparatus

In the following subsections, the various components of the Buckingham-effect apparatus are described, together with explanations of their contribution to the overall experiment.

2.3.1 The optical cascade

Figure 2.1 overleaf contains a schematic of the optical cascade, together with the electronic components which constitute the apparatus. Each component in this schematic will now be discussed in turn.

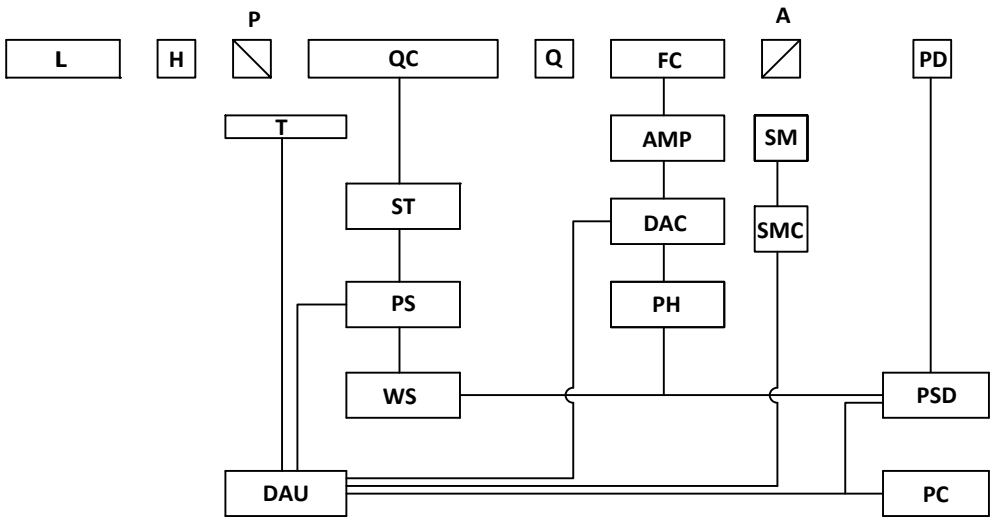

Figure 2.1: Block diagram of the Buckingham-effect apparatus:
L, laser; H, half-wave plate; P, Polarizer; QC, quadrupole cell; Q, quarter-wave plate; FC, water Faraday cell; A, analyzer; PD, photodiode detector; PS, high-voltage power supply; ST, step-up transformer; WS, waveform synthesizer; DAU, data-acquisition and control unit; AMP, power amplifier; DAC, digital-to-analogue converter; PH, phase shifter; SM, stepper motor; SMC, stepper-motor controller; PSD, phase-sensetive detector; PC, personal computer; T, Pt100 RTDs

2.3.2 Laser

The source of the linearly polarized light was a Melles Griot model 25LHP928-230 helium-neon laser rated at 35 mW of output power. The beam had a wavelength of 632.8 nm, a diameter of 1.23 mm at the $\frac{1}{e^2}$ points, and negligible divergence over the approximately 2.5 m distance between source and detector, the manufacturer quoting a divergence of 0.66 mrad. The Rayleigh range of the beam is 7.5 m, while the experimental pathlength is only 2.3 m. Unlike in the earlier work of Couling and Chetty [2, 3], where the shorter optical bench

necessitated the use of two parallel optical rails, with the laser being placed on one rail and its beam steered onto the axis of the other rail using reflecting mirrors, we made use of a new laboratory with a substantially longer optical table, so that the optical train could be placed on one continuous optical rail. This prevented the losses in intensity which accumulate at each reflection.

Figure 2.2: Laser

2.3.3 Half-wave plate and Polarizer

A Newport M-RS65 half-wave plate was placed in between the laser and polarizer, and was rotated so that the plane of polarization of the laser beam coincided with that of the polarizer, thus serving to maximize the intensity of the light arriving at the quadrupole cell entrance window. A Glan-Thompson calcite polarizer prism having an extinction ratio of 1:10^6 was used. It was housed in a divided circle having a resolution of $2^{'}$ of arc. The transmission axis of the polarizer was set to be +45° from vertical for the duration of the experiment.

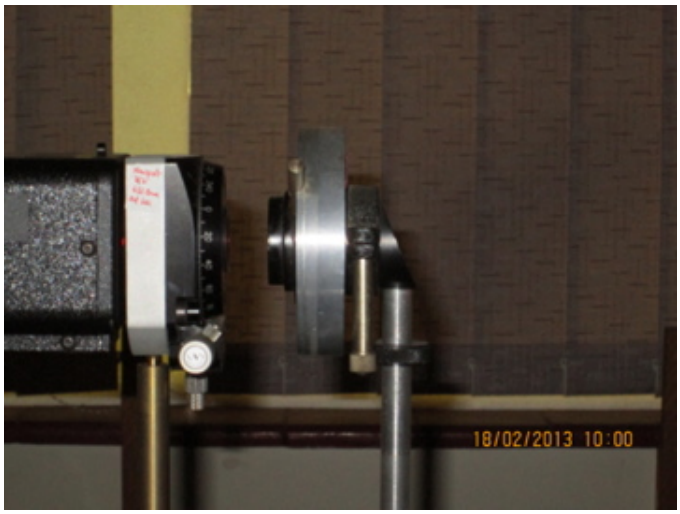

Figure 2.3: Half-wave plate and polarizer prism

2.3.4 Quadrupole cell

The quadrupole cell was comprised of a stainless-steel cylinder of length 2010 mm with an inner diameter of 54.9 mm and a wall thickness of 3.0 mm. Stainless-steel flanges were welded to either end, which allowed for end caps to be attached. These end caps provided the housing for the Pockels glass windows, which were Schott SF57 glass with a diameter of 25.0 mm and a thickness of 5.0 mm. Teflon seals ensured a leak-free seal for the windows even under pressures of 4 MPa. Three pairs of portholes along the length of the cell provided a means for the wire spacing to be measured in situ during an experimental run using a travelling microscope. A pair of stainless-steel wires, each 1800 mm in length and 0.3 mm in diameter, were held fixed in place by two wire holders which were positioned at either end of the cell. There was a tensioning mechanism at one end of the cell by means of which the wires could be set to a reproducible tension with the aid of a calibrated torque wrench. The same high voltage was applied to these wires to generate an electric field gradient between them.

During the early stages of this project, new wire holders were manufactured with a central hole of 1.8 mm in diameter (the previous holders had a central hole 1.0 mm in diameter). This central hole allowed the laser beam to propagate through the birefringent medium. The throughput of the laser light was observed to increase by a factor of five compared to the previous arrangement used by Couling and Chetty [2, 3], and since the sensitivity of the measured

signal increases as the square root of the light intensity, in essence this modification alone has resulted in a doubling of the sensitivity.

The pressure of the gas inside the cell was measured using a Budenberg Master Test Gauge, which had been calibrated using a Budenberg dead-weight tester. The overall accuracy of the measured pressure was ensured to better than 0.1%.

Figure 2.4: The Buckingham (quadrupole) cell

2.3.5 Quarter-wave plate

A Newport model number 05RP04 zero-order quartz quarter-wave plate ($\frac{\lambda}{4}$-plate), with a quoted retardance of $\frac{\pi}{4} \pm 1\%$ at our experimental wavelength of 632.8 nm, was placed after the quadrupole cell exit window. This optical element served to convert the elliptically-polarized light emerging from the birefringent medium back into linearly-polarized light, albeit with a rotation of $\frac{\delta}{2}$ radians from the +45° azimuth. The wave plate was mounted in a divided circle with fine adjustment control and a resolution of $2^{'}$ of arc.

Figure 2.5: The quarter-wave plate mounted in its divided circle

2.3.6 Water Faraday cell

In order to precisely and accurately measure the birefringence induced in a gas sample inside the quadrupole cell, one can cancel it with a nulling device. In the earlier work of Couling and Chetty [2, 3], the nulling device comprised a Farady cell with a 12 cm long cylindrical piece of Pockels glass coaxial with the core of a solenoid. Since this glass was found to attenuate the light passing through it by more than double the attenuation of a Faraday cell with ultra-high-purity water as its rotating medium, we chose to use a water Faraday cell in this work. This has meant a further improvement in the sensitivity of the signal reaching the detector compared to the earlier version of this apparatus. Whereas the previous Faraday cell was calibrated manually, as part of this project, an HPBASIC program was written to automate the calibration procedure, making use of a computer-controlled piezo-driven analyzer rotation stage with closed-loop controller (Newport model CONEX-AG-PR100P). This has allowed for hundreds of calibrations to be gathered and averaged, leading to an order-of-magnitude reduction in the uncertainty associated with the calibration constant, which became $K_F = (0.62280 \pm 0.00068) \times 10^{-6}$ rad mA^{-1}.

Figure 2.6: The water Faraday cell

2.3.7 Analyser prism

The analyzer comprised a Melles Griot Glan-Thompson calcite prism (model PTH112) housed in a Newport model CONEX-AG-PR100P precision rotator. This rotator was a precision piezo-driven device with a closed-loop controller (ensuring a reproducibility of 0.003°), as shown in Figure 2.7. The personal computer controlled the stepper motor via a data-acquisition unit (Agilent model 34907A). The analyzer was offset by a rotation of either $+\varepsilon_1$ or $-\varepsilon_2$ of around 0.5° in magnitude so that a static retardation could be introduced in the optical train, which would facilitate an implementation of Badoz's linear method of optical detection. See Figure 2.8 for an typical experimental plot of the lock-in amplifier output voltage as a function of Faraday cell rms current for the two analyzer offsets.

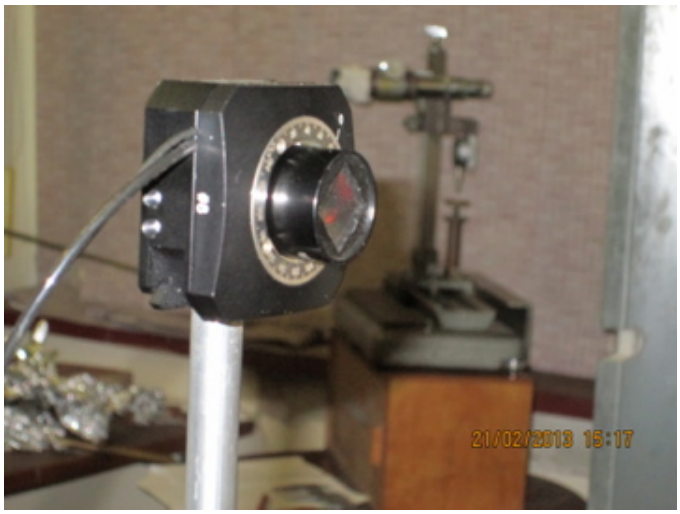

Figure 2.7: The analyzer prism mounted in the Newport computer-controlled precision rotator

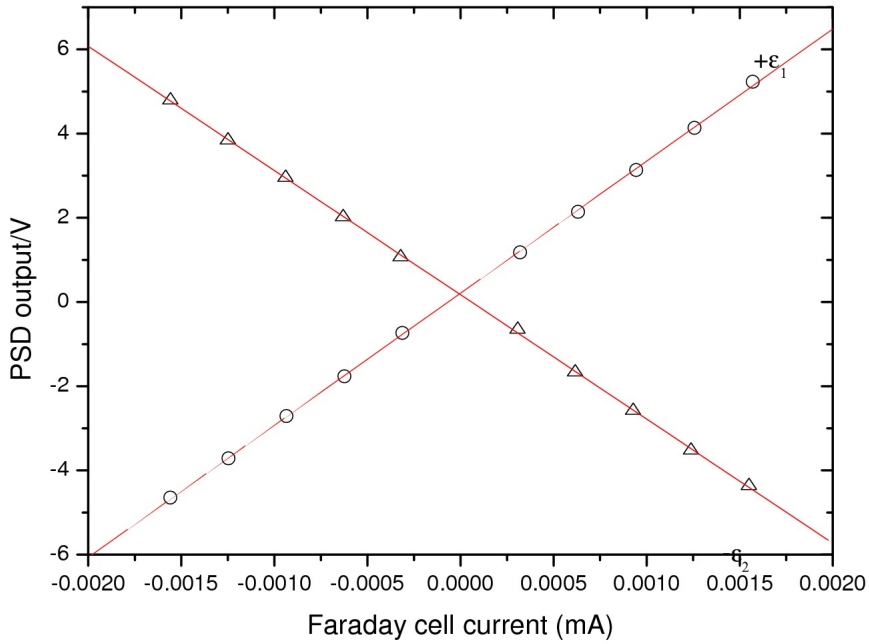

Figure 2.8: An illustrative plot of the phase-sensitive detector (PSD) output voltage as a function of the water Faraday cell (WC) rms current for the small analyzer offsets $+\varepsilon_1$ and $-\varepsilon_2$: he current corresponding to the point of intersection of the two lines is the null current

2.3.8 Modulation system

A Philips model PM5190LF waveform sythesizer was used to generate the sinusoidal ac drive signal which was used to modulate the quadrupole cell as well as the Faraday nulling cell. The high voltage of up to 10 kV required for the quadrupole cell wire electrodes was achieved by means of a 125 W power amplifier which would drive a $1000:1$ turns ratio step-up transformer. By making use of a second (step down) transformer, the high voltage applied to quadrupole cell could be continuously monitored, allowing the voltage output to be maintained at a constant level by means of a feedback loop. This power supply feedback control was completely redesigned as part of this project, employing a PID controller to achieve a voltage stability of better than 0.1%. Appendix A contains a block diagram of the new high voltage controller, together with the controller's schematic and high voltage PID setup.

The nulling Faraday cell was also fed by the waveform generator's primary ac signal, but this first had to pass through a continuously variable phase shift control, allowing the nulling signal to be set precisely in anti-phase to the applied high-voltage, as determined by Lissajous figures displayed on an oscilloscope.

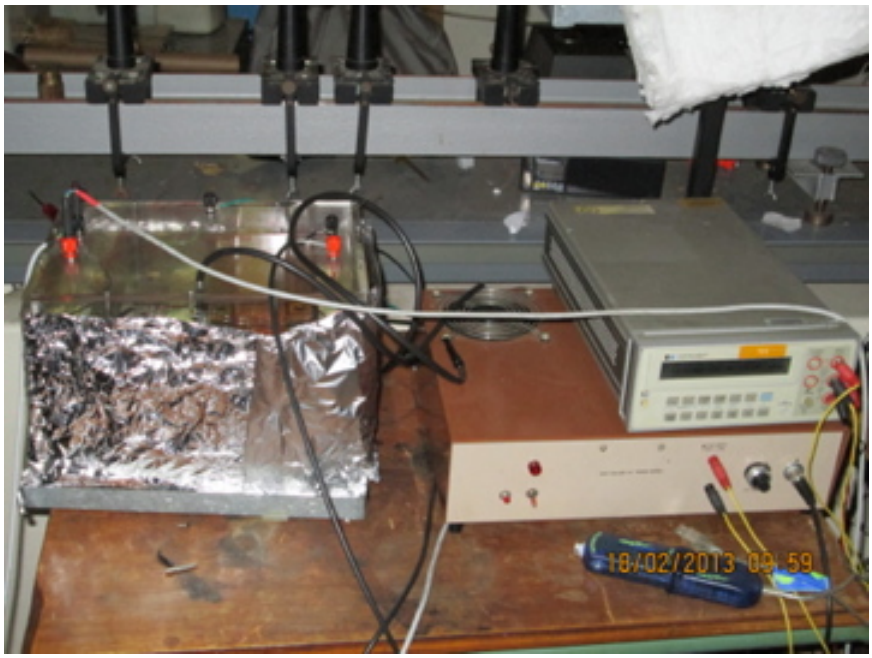

Figure 2.9: The step-up-transformer, high-voltage power supply, and multimeter to monitor the rms applied voltage via the step-down transformer

2.3.9 Detection and data-acquisition system

The light beam emerging from the analyzer was intercepted by a silicon photodiode detector (UDT Sensors model FIL100V0248) which had a high quantum efficiency. The photodiode output voltage was monitored by a Standford Research Systems model SR830 lock-in amplifier. A data-acquisition and control unit (DAU, Agilent model 34970A) was linked to a personal computer via an IEEE interface, allowing for full automation of the experiment both in terms of measurement and of control. A program was coded in HPBasic, which would instruct the unit to record the lock-in amplifier output voltage, the high-voltage applied to quadrupole cell, the room temperature (using a J-type thermocouple, the average temperature inside the oven, and the ac current in the

coils of the Faraday water cell. All measurements were recorded by the DAUs in-built in $6\frac{1}{2}-$digit multimeter. The DAU would also instruct the Newport precision rotator to offset the analyzer by half a degree to $+\epsilon_1$ and $-\epsilon_2$, as required. The DAU also controlled a modified digital-to-analogue converter (DAC, National Semiconductor model DAC0832) to set the rms ac current applied to the Faraday cell's heavy-gauge solenoid coil.

Figure 2.10: The waveform synthersizer, data-acquisition and control unit, oscilloscope, personal computer, lock-in amplifier, phase shifter, digital-to-analogue converter and power amplifier

2.3.10 The oven

A full temperature-dependent study of the EFGIB of a molecular species is essential if the temperature-independent contribution to the induced birefringence (arising from the distortion of electronic structure by the applied electric field gradient) is to be separated from the temperature-dependent term (arising from the partial orientation of the quadrupole moments by the field gradient). Separation of these two contributions is essential if definitive quadrupole moments are to be extracted from EFGIB data, since the temperature-dependent term, though generally quite small, is often not negligible, so that assuming it to make a zero contribution to the EFGIB can lead to errors in the quadrupole moments of up to several percent.

To achieve temperature control of the experiment, an oven was needed to heat up the cell. The oven used in the present study was comprised of a two 2 kW heater elements on either side of the cell, placed inside an oven constructed from two layers of sheet metal interspersed with a 5 cm layer of Fiberfrax insulation. The heater elements were powered off mains, and the temperature control was achieved using an Autonomics TZN4S PID controller. The oven could be heated up to 250°C, and maintained at a particular temperature to within a degree. Three platinum PT100 RTDs served to monitor the temperature inside the oven, being evenly spaced along the length of the cell to obtain an average temperature reading inside the oven.

Figure 2.11: The quadrupole cell oven

Bibliography

[1] A. D. Buckingham and R. L. Disch, *The quadrupole moment of the carbon dioxide molecule,* Proc. R. Soc. Lond. A **273,** 275 (1963).

[2] N. Chetty, Ph. D. thesis, *Measurement of the temperature dependence of the Buckingham effect (electric-field-gradient-induced birefringence) in gases,* University of KwaZulu-Natal (2009).

[3] N. Chetty and V. W. Couling, *Measurement of the electric quadrupole moments of CO_2 and OCS,* Mol. Phys. **109,** 655 (2011).

[4] J. Badoz, *Mesures photoelectriques de faibles birefringences et de tres petits pouvoirs rotatoires,* J. Phys. Radium **17,** A143 (1956).

[5] C. Graham, D. A. Imrie, and R. E. Raab, *Measurement of the electric*

quadrupole moments of CO_2, CO, N_2, Cl_2, and BF_3, Mol. Phys. **93,** 49 (1998).

Chapter 3

Results and discussion

3.1 Carbon dioxide (CO_2)

3.1.1 Introduction

The molecular electric quadrupole moment of carbon dioxide (CO_2) has been the subject of several experimental measurements via the technique of electric-field-gradient-induced birefringence (EFGIB) [1–8]. This method provides a direct route to the molecular quadrupole moment, and if full temperature-dependent measurements are achieved, a definitive quadrupole moment can be extracted. Recent temperature-dependent studies have yielded consistent values for the quadrupole moment of CO_2 [5, 7, 8], so that this property is now well established, and can be used as a useful benchmark in assessing the performance of EFGIB apparatus before experimenting on other species.

Another direct experimental route to the quadrupole moment of CO_2 has been the measurement of the magnetizability anisotropy, $\Delta\chi$, via the Cotton-Mouton effect (CME), which was then coupled with knowledge of the molecular g-value (obtained through molecular-beam magnetic-resonance spectroscopy) [9]. Indirect experimental routes to the molecular quadrupole moment of CO_2, exploiting the effects of intermolecular interactions, have also yielded measured estimates, though these estimates have not always been reliable, mainly due to the assumptions which need to be made [10–21]. Many *ab initio* quantum computational studies have been undertaken for CO_2, the more recent making use of high levels of theory and large basis sets, providing increasingly accurate estimates of the quadrupole moment (see, for example, [22–39]).

We have tested our modified Buckingham-effect apparatus by measuring the EFGIB of CO_2 at room temperature, and checking our measured quadrupole moment for this molecule (applying a correction to ${}_mQ$ for the hyperpolarizability term b) against the best measured and *ab initio* computed data to date.

Our measurements of ${}_mQ$ for carbon dioxide were taken using high-purity Coleman-grade CO_2 (minimum purity 99.99%). The second and third pressure virial coefficients required in the calculations of the molar volumes of the gas samples were obtained from the tabulations of Dymond *et al.* [40]. Refractive indices were calculated from Landolt-Börnstein tables [41] using these molar volumes. The dielectric constant ε_r was calculated using the Clausius-Mosotti function expanded in terms of inverse molar volume,

$$\frac{\varepsilon_r - 1}{\varepsilon_r + 2} V_m = A_\varepsilon + \frac{B_\varepsilon}{V_m} + \frac{C_\varepsilon}{V_m^2} + \cdots , \tag{3.1}$$

where A_ε and B_ε are the first and second dielectric virial coefficients respectively, and V_m is the molar volume. Use was made of the dielectric virial coefficient data measured by Bose and Cole [15]. The 632.8 nm optical-frequency polarizability anisotropy of $\Delta\alpha = (2.350 \pm 0.074) \times 10^{-40}$ C^2 m^2 J^{-1} has been utilized [42].

3.1.2 Results

Twelve experimental runs were performed at room temperature, and the ${}_mQ$ value for each run was corrected for the hyperpolarizability term $b = (-0.34 \pm 0.19) \times 10^{-60}$ C^3 m^4 J^{-2} as measured previously [8], thus yielding an accurate quadrupole moment Θ via equation 1.9. The data are presented in Table 3.1, where the uncertainties provided are the standard deviations associated with the measured quantities. These data yield a quadrupole moment of $\Theta = (-14.30 \pm 0.73) \times 10^{-40}$ C m^2, where this final uncertainty is a combination of maximum errors and standard deviations, as described in detail in section 3.2.2 for the new work on the oxygen molecule. This quadrupole moment is in excellent agreement with the values extracted from full temperature-dependent studies, namely $\Theta = (-14.31 \pm 0.74) \times 10^{-40}$ C m^2 [7, 8] and $\Theta = (-14.27 \pm 0.63) \times 10^{-40}$ C m^2 [5].

Table 3.1: The Buckingham constant ($_mQ$) values and electric quadrupole moments (Θ) for molecular carbon dioxide measured at room temperature and at a wavelength of 632.8 nm

$\overline{T}$ (K)	P (MPa)	$10^4 V_m$ ($m^3\,mol^{-1}$)	ε_r	$10^6(n-1)$	$10^{26}\,{}_mQ$ ($C\,m^5\,J^{-1}\,mol^{-1}$)	$10^{40}\,\Theta$ ($C\,m^2$)
296.5	2.004	1.0935	1.0205	9114	-25.64 ± 0.22	-14.33 ± 0.81
296.9	2.007	1.0944	1.0205	9107	-25.35 ± 0.19	-14.18 ± 0.79
297.5	2.012	1.0942	1.0205	9108	-25.69 ± 0.18	-14.41 ± 0.79
296.9	2.006	1.0948	1.0205	9103	-25.51 ± 0.22	-14.28 ± 0.81
297.0	2.007	1.0947	1.0205	9104	-25.60 ± 0.21	-14.33 ± 0.80
297.4	2.010	1.0954	1.0204	9099	-25.66 ± 0.22	-14.39 ± 0.81
297.0	2.007	1.0944	1.0205	9107	-25.39 ± 0.18	-14.21 ± 0.78
296.3	2.003	1.0938	1.0205	9111	-25.53 ± 0.18	-14.26 ± 0.79
296.8	2.005	1.0946	1.0205	9105	-25.59 ± 0.24	-14.31 ± 0.82
297.1	2.007	1.0955	1.0204	9097	-25.68 ± 0.17	-14.38 ± 0.78
297.1	2.006	1.0959	1.0204	9094	-25.49 ± 0.19	-14.27 ± 0.79
296.9	2.005	1.0955	1.0204	9098	-25.59 ± 0.23	-14.32 ± 0.82
					mean	-14.30 ± 0.73

3.1.3 Discussion

A tabulation of our measured quadrupole moment for CO_2, together with experimental and *ab initio* computed values obtained by other researchers, is presented in Table 3.2. The excellent agreement obtained with the data of other researchers leads us to conclude that our modified Buckingham-effect apparatus is yielding precise and accurate measured EFGIB data, so that we can confidently proceed with measurements of molecular oxygen.

Table 3.2: A comparison of selected molecular electric quadrupole moments for CO_2

$10^{40}\Theta$ (C m^2)	Method	Reference
-14.30 ± 0.73	EFGIB (single temp., corrected for $b = (-0.34 \pm 0.19 \times 10^{-60}$ C^3 m^4 J^{-2})	this work
-14.31 ± 0.74	EFGIB (temp. dependent)	[7, 8]
-14.27 ± 0.63	EFGIB (temp. dependent)	[5]
-14.98 ± 0.5	EFGIB (temp. dependent)	[3]
-13.9 ± 0.22	EFGIB (single temp., $b = 0$)	[6]
-13.56 ± 0.48	EFGIB (single temp.[6], corrected in [8] for $b = -0.34 \times 10^{-60}$ C^3 m^4 J^{-2} and ϵ_r)	[6, 8]
-14.0 ± 0.8	magnetic anisotropy	[9]
-13.7	viscosities & pressure virial coefficients	[14]
-14.4	dielectric & pressure virial coefficients	[15]
-14.94 ± 0.1	dielectric & pressure virial coefficients	[21]
-14.3 ± 1.3	collision-induced far IR absorption	[19]
-15.2 ± 1.0	MCSCF computation	[24]
-14.3	BD(T) computation	[30]
-14.29 ± 0.09	CCSD(T) computation	[32]
-14.34	CCSD(T) computation	[35]
-14.31	CCSD(T) computation	[36]
-14.29	CCSD(T) computation	[39]

3.2 Oxygen (O_2)

3.2.1 Introduction

Only one previous EFGIB measurement of the molecular electric quadrupole moment of oxygen exists, and it was performed at room temperature by Buckingham and co-workers in 1968 [2].

Our measurements of ${}_mQ$ for molecular oxygen were taken using ultra-high-purity O_2, with a quoted 99.998% minimum purity, supplied by Afrox. The second and third pressure virial coefficients which are required in the calculation of the molar volumes of the gas samples were obtained from the tabulations of Dymond *et al.* [40]. Refractive indices were calculated from Landolt-Börnstein tables [41] using these molar volumes. The dielectric constant ε_r was calculated using the correlation

$$\frac{\varepsilon_r - 1}{\varepsilon_r + 2} = A_{\varepsilon,273\,\mathrm{K}}\,\rho\left(1 + b_\varepsilon\,\rho + c_\varepsilon\,\rho^2\right) + A_\tau\,\rho\left(\frac{T}{273.16\,\mathrm{K}} - 1\right) \tag{3.2}$$

as deduced by Schmidt and Moldover [43], where ρ is the molar density. Here, the term with the parameter A_τ accounts for the small temperature dependence of A_ε arising from centrifugal stretching in diatomic molecules. The parameters which we have used in Eq. (3.2) are taken from recent high-precision ε_r measurements of O_2 at 273 K, 293 K and 323 K, namely $A_{\varepsilon,273\mathrm{K}} = 3.95760\ \mathrm{cm}^3$

mol^{-1}, $b_\varepsilon = 0.16\,\mathrm{cm}^3\,\mathrm{mol}^{-1}$, $c_\varepsilon = -50\,\mathrm{cm}^6\,\mathrm{mol}^{-2}$, and $A_\tau = 0.0037\,\mathrm{cm}^3\,\mathrm{mol}^{-1}$ [44].

The polarizability anisotropy of $\Delta\alpha = 1.223\times10^{-40}\,\mathrm{C}^2\,\mathrm{m}^2\,\mathrm{J}^{-1}$ used here was obtained by Bridge and Buckingham from measurements of the low-density depolarization ratio ρ_0 of Rayleigh-scattered light performed at the wavelength 632.8 nm [45]. To estimate the uncertainty in $\Delta\alpha$, the classical expression

$$\rho_0 = \frac{3(\Delta\alpha)^2}{45\alpha^2 + 4(\Delta\alpha)^2} \tag{3.3}$$

which relates ρ_0 to $\Delta\alpha$ and the mean dynamic polarizability α can be conveniently recast as

$$\Delta\alpha = 3\alpha\sqrt{\frac{5\rho_0}{3-4\rho_0}}. \tag{3.4}$$

Bridge and Buckingham obtained $100\rho_0 = (3.02 \pm 0.01)$ for O_2, and estimated an uncertainty of 0.5% for the $\alpha = 1.778\times10^{-40}\,\mathrm{C}^2\,\mathrm{m}^2\,\mathrm{J}^{-1}$ which they used in their analysis, so that their $\Delta\alpha$ deduced via Eq. (3.4) would have an uncertainty of 0.7%. The high-precision $\alpha = (1.7803 \pm 0.0003)\times10^{-40}\,\mathrm{C}^2\,\mathrm{m}^2\,\mathrm{J}^{-1}$ recently measured for O_2 at 632.99 nm by Hohm [46] lies within 0.13% of the value used by Bridge and Buckingham, improving the uncertainty of this component of

Eq. (3.4). Unfortunately, the only other depolarization ratio measured for O_2 at 632.8 nm, namely the $100\rho_0 = (2.9 \pm 0.1)$ obtained by Baas and van den Hout [47], is some 4.2% smaller than Bridge and Buckingham's value. As Bogaard *et al.* have argued [42], while the precision of a set of ρ_0 values measured by a given investigator can be as high as 0.5% or better, the determinations of different investigators can be discrepant by as much as 4%, so that the accuracy of depolarization ratios is assumed to be no better than $\approx \pm 3\%$. The uncertainty in the $\Delta\alpha$ of Bridge and Buckingham is consequently estimated to be around 2.3%, arising from 0.2% in α, and 2.1% in $\sqrt{5\rho_0/(3-4\rho_0)}$ (as compared with the Baas and van den Hout measurement). It should be noted that the *ab initio* calculated $\Delta\alpha = 1.184 \times 10^{-40}$ C^2 m^2 J^{-1} at 632.8 nm of Jonsson *et al.* [48] lies closer to the $\Delta\alpha = 1.19 \times 10^{-40}$ C^2 m^2 J^{-1} obtained by Baas and van den Hout. This MCSCF computation includes zero-point vibrational averaging. The Bridge and Buckingham $\Delta\alpha$ has been used in the extraction of Θ from Eq. (1.12) since their depolarization ratio has a statistical uncertainty an order of magnitude smaller than that of Baas and van den Hout, indicating a greater precision of measurement. However, there remains ambiguity as to which of the two ρ_0 values is the more accurate, and so the the Baas and van den Hout $\Delta\alpha$ is used to calculate a Θ for comparative purposes. It would appear that fresh light-scattering measurements of O_2 are warranted to bring resolution to this ambiguity.

3.2.2 Results

Several experimental runs were performed at room temperature, and the ${}_mQ$ value for each run, together with the deduced quadrupole moment Θ (assuming $b' = 0$), are presented in Table 3.3 and Table 3.4. After the ten measurements in Table 3.3 were obtained, the quadrupole cell was completely dismantled and reassembled with a new set of wire electrodes. The five measurements in Table 3.4 were then recorded. The uncertainities provided in the two tables are the standard deviations associated with the measured quantities. The possible sources of systematic error in the measured quantities have been reported in the paper by Chetty and Couling [8], and arise from the determination of the absolute temperature of the gas (0.2%), the molar volume of the gas (0.3%), the length of the wires in the cell (0.1%), the on-axis electric field gradient (0.4%), and the calibration constant of the Faraday nulling cell (now reduced to 0.2%). The uncertainty in the polarizability anisotropy used in the analysis (2.3%) must also be taken into account. The final uncertainty ascribed to the deduced mean Θ is a combination of maximum errors and standard deviations, as proposed by Baird [49], this final uncertainty denoting an interval over which the probability of finding the true quadrupole moment is estimated to be two-thirds.

The measurements in Table 3.3 yield a quadrupole moment of $\Theta = (-1.034 \pm 0.027) \times 10^{-40}$ C m^2, while those in Table 3.4 yield $\Theta = (-1.033 \pm 0.027) \times 10^{-40}$ C m^2. The combined 15 measurements yield a quadrupole moment of $\Theta =$

$(-1.033 \pm 0.027) \times 10^{-40}\,\mathrm{C\,m^2}$.

If the $\Delta\alpha$ of Baas and van den Hout (together with its uncertainty quoted in [47]) is used instead of that of Bridge and Buckingham, the combined 15 measurements yield a quadrupole moment of $\Theta = (-1.062 \pm 0.042) \times 10^{-40}\,\mathrm{C\,m^2}$.

Table 3.3: The Buckingham constant (${}_mQ$) values and electric quadrupole moments (Θ) for molecular oxygen measured at room temperature and at a wavelength of 632.8 nm

$\overline{T}$ (K)	$f(\overline{T})$	P (MPa)	$10^4 V_m$ ($m^3\,mol^{-1}$)	ε_r	$10^6(n-1)$	$10^{26}\,{}_mQ$ ($C\,m^5\,J^{-1}\,mol^{-1}$)	$10^{40}\,\Theta$ ($C\,m^2$)
298.7	0.9931	2.715	8.996	1.0133	6675	-0.939 ± 0.034	-1.047 ± 0.070
298.6	0.9931	2.710	9.011	1.0132	6664	-0.920 ± 0.026	-1.026 ± 0.060
298.3	0.9931	2.705	9.016	1.0132	6660	-0.930 ± 0.029	-1.036 ± 0.064
298.5	0.9931	2.702	9.037	1.0132	6645	-0.939 ± 0.028	-1.047 ± 0.063
298.4	0.9931	2.696	9.053	1.0132	6633	-0.908 ± 0.030	-1.012 ± 0.064
298.2	0.9931	2.693	9.056	1.0132	6631	-0.910 ± 0.026	-1.021 ± 0.060
298.2	0.9931	2.681	9.095	1.0131	6602	-0.936 ± 0.022	-1.042 ± 0.056
297.9	0.9931	2.668	9.133	1.0131	6575	-0.934 ± 0.033	-1.039 ± 0.068
298.2	0.9931	2.663	9.159	1.0130	6557	-0.937 ± 0.026	-1.044 ± 0.061
297.8	0.9931	2.653	9.182	1.0130	6540	-0.920 ± 0.031	-1.023 ± 0.066
						mean	-1.034 ± 0.027

Table 3.4: The Buckingham constant ($_mQ$) values and electric quadrupole moments (Θ) for molecular oxygen measured at room temperature and at a wavelength of 632.8 nm after complete dismantling and reassembly of the cell and electrode array

$\overline{T}$ (K)	$f(\overline{T})$	P (MPa)	$10^4 V_m$ ($m^3\,mol^{-1}$)	ε_r	$10^6(n-1)$	$10^{26}\,{}_mQ$ ($C\,m^5\,J^{-1}\,mol^{-1}$)	$10^{40}\,\Theta$ ($C\,m^2$)
298.6	0.9931	2.708	9.043	1.0132	6640	-0.929 ± 0.064	-1.038 ± 0.103
300.2	0.9931	2.723	9.018	1.0132	6659	-0.920 ± 0.044	-1.031 ± 0.081
300.2	0.9931	2.722	9.021	1.0132	6657	-0.912 ± 0.082	-1.022 ± 0.123
300.5	0.9931	2.724	9.031	1.0132	6649	-0.929 ± 0.058	-1.038 ± 0.096
300.6	0.9931	2.720	9.041	1.0132	6642	-0.921 ± 0.064	-1.034 ± 0.103
						mean	-1.033 ± 0.027

3.2.3 Discussion

This EFGIB investigation has yielded a molecular electric quadrupole moment of $\Theta = (-1.033 \pm 0.027) \times 10^{-40}$ C m^2 for O_2. Since the measurements were obtained at room temperature, the extraction of the quadrupole moment Θ from the measured ${}_mQ$ data via Eq. (1.12) has been achieved by assuming the b' contribution to be negligible, i.e. setting b' to zero.

Only one previous EFGIB determination of Θ for O_2 exists, undertaken at room temperature by Buckingham *et al.*, and yielding $\Theta = (-1.33 \pm 0.33) \times 10^{-40}$ C m^2 [2]. Here, the uncertainty is 25%, and the b' term has been assumed to be zero. Cohen and Birnbaum have obtained Θ for O_2 using the indirect approach of analyzing pressure-induced far-infrared spectra [50]. These results are dependent on the model used to describe the intermolecular interaction potential, and are generally not considered to be particularly reliable. For O_2 they obtained $\Theta = |1.1| \times 10^{-40}$ C m^2, which is in reasonable agreement with our value.

The temperature-independent b'-term's contribution to the induced birefringence of small molecules has been found to range from around 3% for CO_2 [7] up to 10% for N_2 [51]. Clearly, this term typically makes a small but non-negligible contribution to the EFGIB, and so needs to be accounted for if a definitive quadrupole moment is to be extracted from the measured data. This can be achieved in one of two ways: either a full temperature-dependent experimental study can be undertaken, so that the temperature-independent

and temperature-dependent contributions to ${}_mQ$ can be separated out; or the b' term can be calculated by *ab initio* quantum computational techniques, allowing for Θ to be accurately extracted from ${}_mQ$ using Eq. (1.12).

The measured ${}_mQ$ of O_2 is extraordinarily tiny, being some 28 times smaller than the CO_2 ${}_mQ$ at room temperature, and a consequence of this has been an inability to realize measurements of ${}_mQ$ for O_2 at higher temperatures using our current experimental arrangement. While a full temperature-dependent study of the Buckingham effect for O_2 is desirable, considerable experimental challenges will need to be overcome before this can be realized.

A tabulation of our quadrupole moment for O_2, together with selected values obtained by other researchers, is provided in Table 3.5. Here we see that earlier *ab initio* calculations of Θ have tended to yield larger absolute values than the most recent $\Theta = -1.010 \times 10^{-40}$ C m^2 obtained by Bartolomei *et al.*, which has been attributed to the lack of dynamic electron correlation in the previous calculations [59]. Since the ground state of molecular oxygen is a triplet, a multi-reference type wavefunction is required, presenting a significant challenge in the undertaking of *ab initio* computations for this species. The *ab initio* calculations of Bartolomei *et al.* are performed at the multiconfigurational self-consistent field (MCSCF) level of theory, and include methods which account for dynamic electron correlation effects, such as the multireference averaged coupled pair functional (ACPF) theory. Their preferred value is 2.3% larger (less negative) than our experimental value, the agreement being quite

Table 3.5: A comparison of selected molecular electric quadrupole moments for O_2

$10^{40}\Theta$ (C m^2)	Method	Reference
-1.033 ± 0.027	EFGIB (single temp., $b' = 0$)	this work
-1.33 ± 0.33	EFGIB (single temp., $b' = 0$)	[2]
-1.0	Pressure-induced far IR spectrum	[52, 53]
-1.13 ± 0.04	Pressure-induced far IR spectrum	[50]
-1.184	MCSCF computation	[54]
-1.218	CI-perturbation computation	[55]
-1.185	RAS computation	[56]
-1.020	CBS-CASSCF+1+2 computation	[57]
-1.140	MCSCF computation	[58]
-1.010	ACPF computation†	[59]

† this is considered to be the most reliable *ab initio* computation to date

good. It should be noted that Bartolomei *et al.* have not included vibrational corrections in their computed Θ, which could partially account for the small discrepancy between experiment and theory.

If theoreticians pursue *ab initio* computations of the b' term for this molecule, it will be interesting to see whether correction of our measured Θ brings the experimental and calculated quadrupole moments of O_2 into better agreement. The effect of inclusion of vibrational averaging in the *ab initio* computation of Θ itself would also be worth examining.

This project will be pursued further at the PhD level, where efforts to complete a full temperature-dependent study of the EFGIB of O_2 will be undertaken. If accomplished, this will serve to estimate the hyperpolarizability term b and hence its contribution to the EFGIB. This will allow for the extraction of a definitive quadrupole moment from the experimental data.

Bibliography

[1] A. D. Buckingham and R. L. Disch, *The quadrupole moment of the carbon dioxide molecule*, Proc. R. Soc. Lond. A **273,** 275 (1963).

[2] A. D. Buckingham, R. L. Disch, and D. A. Dunmur, *The quadrupole moments of some simple molecules*, J. Am. Chem. Soc. **90,** 3104 (1968).

[3] M. R. Battaglia, A. D. Buckingham, D. Neumark, R. K. Pierens, and J. H. Williams, *The quadrupole-moments of carbon-dioxide and carbon-disulfide*, Mol. Phys. **43,** 1015 (1981).

[4] C. Graham, J. Pierrus, and R. E. Raab, *Measurement of the electric quadrupole-moments of CO_2, CO and N_2*, Mol. Phys. **67,** 939 (1989).

[5] J. N. Watson, I. E. Craven, and G. L. D. Ritchie, *Temperature dependence of*

electric field-gradient induced birefringence in carbon dioxide and carbon disulfide, Chem. Phys. Lett. **274,** 1 (1997).

[6] C. Graham, D. A. Imrie, and R. E. Raab, *Measurement of the electric quadrupole moments of CO_2, CO, N_2, Cl_2 and BF_3*, Mol. Phys. **93,** 49 (1998).

[7] N. Chetty, Ph. D. thesis, *Measurement of the temperature dependence of the Buckingham effect (electric-field-gradient-induced birefringence) in gases*, University of KwaZulu-Natal (2009).

[8] N. Chetty and V. W. Couling, *Measurement of the electric quadrupole moments of CO_2 and OCS*, Mol. Phys. **109,** 655 (2011).

[9] H. Kling and W. Hüttner, *The temperature-dependence of the Cotton-Mouton effect of N_2, CO, N_2O, CO_2, OCS and CS_2 in the gaseous state*, Chem. Phys. **90,** 207 (1984).

[10] D. R. Johnston and R. H. Cole, *Dielectric constants of imperfect gases. II. Carbon dioxide and ethylene*, J. Chem. Phys. **36,** 318 (1962).

[11] R. H. Orcutt, *Influence of molecular quadrupole moments on the second virial coefficient,* J. Chem. Phys. **39,** 605 (1963).

[12] A. A. Maryott and S. J. Kryder, *Collision-induced microwave absorption in compressed gases. III. CO_2-foreign-gas mixtures,* J. Chem. Phys. **41,** 1580 (1964).

[13] M. Bloom, I. Oppenheim, M. Lipsicas, C. G. Wade, and C. F. Yarnell, *Nuclear spin relaxation in gases and liquids. IV. Interpretation of experiments in gases,* J. Chem. Phys. **43,** 1036 (1965).

[14] T. H. Spurling and E. A. Mason, *Determination of molecular quadrupole moments from viscosities and second virial coefficients,* J. Chem. Phys. **46,** 322 (1967).

[15] T. K. Bose and R. H. Cole, *Dielectric and pressure virial coefficients of imperfect gases. 2. CO_2-argon mixtures,* J. Chem. Phys. **52**, 140 (1970).

[16] J. E. Harries, *The quadrupole moment of CO_2, measured from the far infrared spectrum,* J. Phys. B **3,** L150 (1970).

[17] K. K. Datta and Y. Singh, *Molecular multipole moments determined from viscosity and second virial coefficients*, J. Chem. Phys. **55,** 1028 (1971).

[18] W. H. Flygare and R. C. Benson, *The molecular Zeeman effect in diamagnetic molecules and the determination of molecular magnetic moments (g-values), magnetic susceptibilities, and molecular quadrupole moments*, Mol. Phys. **20,** 225 (1971).

[19] W. Ho, G. Birnbaum and A. Rosenberg, *Far-infrared collision-induced absorption in CO_2. 1. temperature depencence*, J. Chem. Phys. **55,** 1028 (1971).

[20] U. Borkenhagen, H. Malthan and J. Peter Toennies, *Molecular beam measurements of inelastic cross sections for transitions between defined rotational states (j,m) of CsF in collisions with He, Ne, Ar, Kr, CH4, CF_4, SF_6, C_2H_6, N_2, CO, CO_2, N_2O, CH_3Cl, CH_3Br, CF_3H, and CF_3Br*, J. Chem. Phys. **71,** 1722 (1979).

[21] A. Hourri, J. M. St-Arnaud and T. K. Bose, *Dielectric and pressure virial*

coefficients of imperfect gases: CO_2-SF_6 mixtures, J. Chem. Phys. **106,** 1780 (1997).

[22] T. D. Gierke, H. L. Tigelaar, and W. H. Flygare, *Calculation of molecular electric dipole and quadrupole moments*, J. Am. Chem. Soc. **94,** 330 (1972).

[23] W. H. Flygare, *Magnetic interactions in molecules and an analysis of molecular electronic charge distribution from magnetic parameters*, Chem. Rev. **74,** 653 (1974).

[24] R. D. Amos and M. R. Battaglia, *Molecular quadrupole moments, magnetizability, nuclear magnetic shielding and spin-rotation tensors of CO_2, OCS and CS_2*, Mol. Phys. **36,** 1517 (1978).

[25] A. J. Stone and M. Alderton, *Distributed multipole analysis - methods and applications*, Mol. Phys. **56,** 1047 (1985).

[26] J. Sadlej and B. O. Roos, *A quantum chemical study of the hydrogen-bonding in the $CO_2 \cdots HF$ and $N_2O \cdots HF$ complexes*, Theor. Chim. Acta **76,** 173 (1989).

[27] M. A. Spackman, *Accurate prediction of static dipole polarizabilities with moderately sized basis sets,* J. Phys. Chem. **93,** 7594 (1989).

[28] G. Maroulis and A. J. Thakkar, *Polarizabilities and hyperpolarizabilities of carbon-dioxide*, J. Chem. Phys. **93,** 4164 (1990).

[29] K. E. Laidig, *The atomic origins of the quadrupole and second moments in the series CO_2, OCS, and CS_2*, Chem. Phys. **163,** 287 (1992).

[30] A. J. Russell and M. A. Spackman, personal communication to G. L. D. Ritchie [5]

[31] G. L. Gutsev, R. J. Bartlett, and R. N. Compton, *Electron affinities of CO_2, OCS, and CS_2*, J. Chem. Phys. **108,** 6756 (1998).

[32] S. Coriani, A. Halkier, A. Rizzo and K. Ruud, *On the molecular electric quadrupole moment and the electric-field-gradient-induced birefringence of CO_2 and CS_2*, Chem. Phys. Lett. **326,** 269 (2000).

[33] R. Glaser, Z. Wu, and M. Lewis, *A higher level ab initio quantum-*

mechanical study of the quadrupole moment tensor components of carbon dioxide, J. Mol. Struct. **556,** 131 (2000).

[34] J. M. Junquera-Hernández, J. Sánchez-Marín, and D. Maynau, *Molecular electric quadrupole moments calculated with matrix dressed SDCI*, Chem. Phys. Lett. **359,** 343 (2002).

[35] B. T. Chang, O. Akin-Ojo, R. Bukowski, K. Szalewicz, S. A. Kucharski, H. L. Williams, and B. M. Rice, *Potential energy surface and rovibrational spectrum of He-N_2O dimer*, J. Chem. Phys. **119,** 11654 (2003).

[36] G. Maroulis, *Electric (hyper)polarizability derivatives for the symmetric stretching of carbon dioxide*, Chem. Phys. **291,** 81 (2003).

[37] G. Maroulis, *A note on the electric multipole moments of carbon dioxide*, Chem. Phys. Lett. **396,** 66 (2004).

[38] M. Singh, K. Leonhard, and K. Lucas, *Making equation of state models predictive Part 1: Quantum chemical computation of molecular properties*, Fluid Phase Equilib. **258,** 16 (2007).

[39] A. L. Mullen, T. Pham, K. A. Forrest, C. R. Cioce, K. McLaughlin, and B. Space, *A polarizable and transferable PHAST CO_2 potential for materials simulation*, J. Chem. Theory Comput. **9,** 5421 (2013).

[40] J. H. Dymond, K. N. Marsh, R. C. Wilhoit, and K. C. Wong, *The virial coefficients of pure gases and mixtures* (Springer-Verlag, Berlin, 2002).

[41] Landolt-Börnstein, Zahlenwerte und Funktionen, edited by K.-H. Hellwege and A. M. Hellwege (Springer-Verlag, Berlin, 1962) Band II, Teil 8.

[42] M. P. Bogaard, A. D. Buckingham, R. K. Pierens, and A. H. WHite, *Measurements of depolarization ratios and polarizability anisotropies of gaseous molecules*, J. Chem. Faraday Trans. 1 **74,** 3008 (1978).

[43] J. W. Schmidt and M. R. Moldover, *Dielectric permittivity of eight gases measured with cross capacitors*, Int. J. Thermophys. **24,** 375 (2003).

[44] E. F. May, M. R. Moldover, and J. W. Schmidt, *Electric and magnetic susceptibilities of gaseous oxygen: Present data and modern theory compared*, Phys. Rev. A **78,** 032522 (2008).

[45] N. J. Bridge and A. D. Buckingham, *The polarization of laser light scattered by gases*, Proc. Roy. Soc. London Ser. A **295,** 334 (1966).

[46] U. Hohm, *Frequency-dependence of 2nd refractivity virial-coefficients of small molecules between 325 nm and 633 nm*, Mol. Phys. **81,** 157 (1994).

[47] F. Baas and K. D. van den Hout, *Measurements of depolarization ratios and polarizability anisotropies of gaseous molecules*, Physica A **95,** 597 (1979).

[48] D. Jonsson, P. Norman, O. Vahtras, H. Ågren, and A. Rizzo, *The hypermagnetizability of molecular oxygen*, J. Chem. Phys. **106,** 8552 (1997).

[49] D.C. Baird, *Experimentation: an introduction to measurement theory and design* (Prentice Hall, Englewood Cliffs NJ, 1964).

[50] E. R. Cohen and G. Birnbaum, *Influence of potential function on determination of multipole moments from pressure-induced far-infrared spectra*, J. Chem. Phys. **66,** 2443 (1977).

[51] G. L. D. Ritchie, J. N. Watson, and R. I. Keir, *Temperature dependence of electric field-gradient induced birefringence (Buckingham effect) and*

molecular quadrupole moment of N_2. Comparison of experiment and theory, Chem. Phys. Lett. **370,** 376 (2003).

[52] D. R. Bosomworth and H. P. Gush, *Collision-induced absorption of compressed gases in far infrared*, Can. J. Phys. **43,** 751 (1965).

[53] M. Evans, *Some equations for multipole-induced dipole absorption in linear molecules*, Mol. Phys. **29,** 1345 (1975).

[54] J. H. van Lenthe and F. B. van Duijneveldt, *Ab initio calculations of the He-O_2 potential energy surface. Hartree-Fock instability of O_2*, J. Chem. Phys. **81,** 3168 (1984).

[55] W. Rijks, M. van Heeringen, and P. E. S. Wormer, *The frequency-dependent polarizability of O_2 and the dispersion interaction in dimers containing O_2 from a single, double, triple configuration interaction perturbation approach*, J. Chem. Phys. **90,** 6501 (1989).

[56] H. Hettema, P. E. S. Wormer, P. Jørgensen, H. J. Aa. Jensen, and T. Helgaker,

Frequency-dependent polarizabilities of O_2 and van der Waals coefficients of dimers containing O_2, J. Chem. Phys. **100,** 1297 (1994).

[57] D. B. Lawson and J. F. Harrison, *Distance dependence and spatial distribution of the molecular quadrupole moments of H_2, N_2, O_2, and F_2*, J. Phys. Chem. A **101,** 4781 (1997).

[58] B. F. Minaev, *Ab initio study of the ground state properties of molecular oxygen*, Spectrochim. Acta A **60,** 1027 (2004).

[59] M. Bartolomei, E. Carmona-Novillo, M. I. Hernández, J. Campos-Martínez, and R. Harnández-Lamoneda, *Long-range interaction for dimers of atmospheric interest: dispersion, induction and electrostatic contributions for O_2-O_2, N_2-N_2 and O_2-N_2*, J. Comp. Chem. **32,** 279 (2011).

Appendix A

High voltage controller block diagram, PID setup and controller schematic

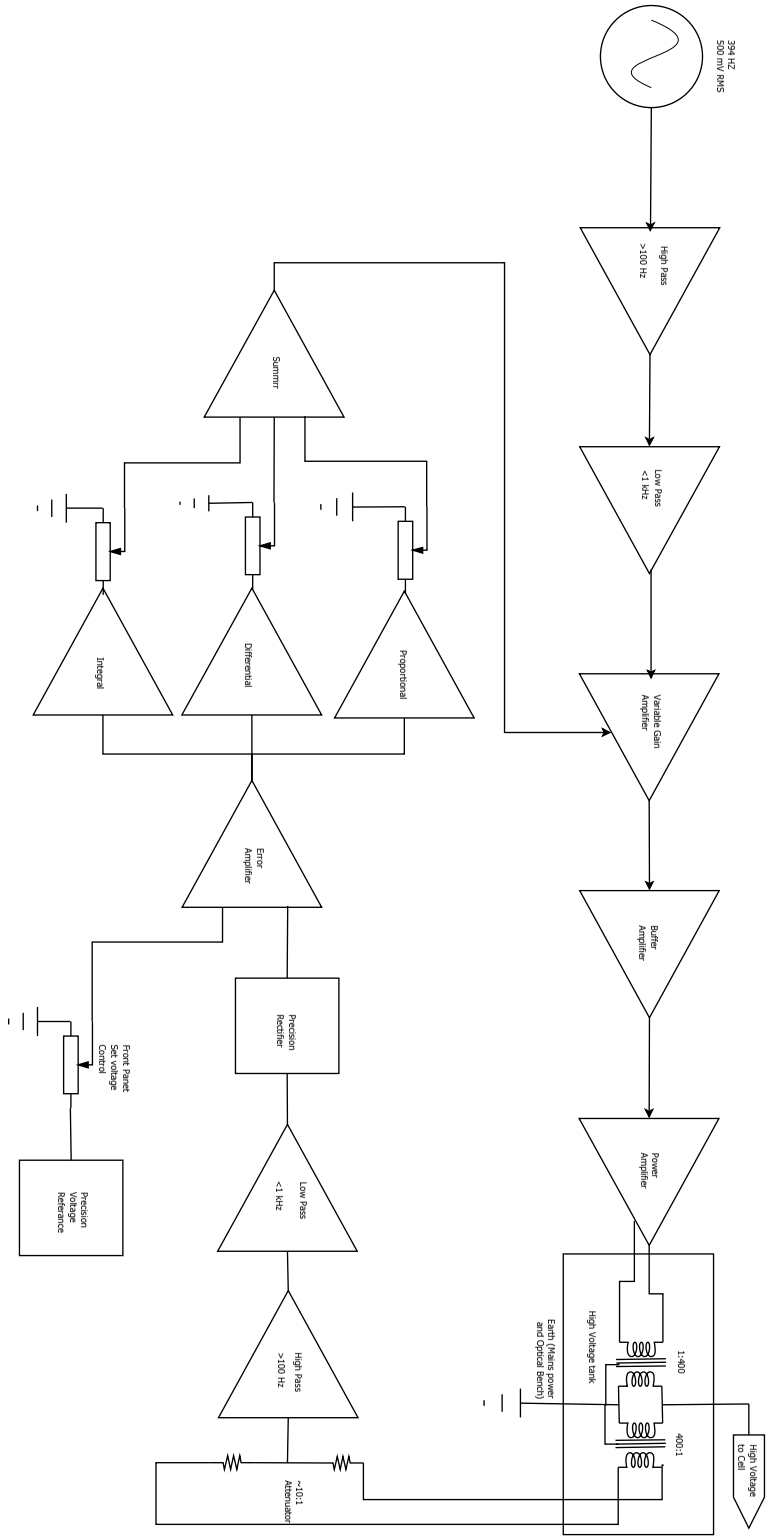
394 HZ
500 mV RMS
High Pass
>100 Hz
Low Pass
<1 kHz
Variable Gain
Amplifier
Buffer
Amplifier
Power
Amplifier
High Voltage tank
1:400
400:1
Earth (Mains power
and Optical bench)
High Voltage
to Cell
~10:1
Attenuator
High Pass
>100 Hz
Low Pass
<1 kHz
Precision
Rectifier
Error
Amplifier
Integral
Differential
Proportional
Summmr
Front Panel
Set voltage
Control
Precision
Voltage
Reference

Monitor Gain
Adjust for 1V per kV
At monitor output
(Power Amplifier
must be enabled
and input signal
should be between
200 and 500 mV RMS.)
Adjust 180 K resistor
if necessary.
(180 K correct for
1 : 400 Transformer)
Panel Trim
Adjust So that 10 turn
front panel control
matches output voltage.
Adjust 240 Ω and
Parallel not fitted
resistor if necessary.
(240 Ω is correct
for 1 : 400 transformer.)
Panel Trim
100E10T
Voltage Set
Potentiometer
1K 10T
Monitor Gain
100K10T
Monitor Zero
100E10T
Feedback
Input
Output
Voltage monitor
Prop.
1K0
Diff.
1K0
Integral
1K0
Proportional
Increase until
System just
starts to
oscillate
Back off to
~ 80% of this
Value.
Differential
After adjusting
Prop and Int .
Adjust for best
recovery from
a step change
in load.
(Disconnect a
10 to 40 W
Lamp across
transformer)
Integral
After adjusting
Proportional gain
Set output to 0
(Front panel control)
Increase Integralf.
gain until output
goes to a low
value.
Monitor Zero
Adjust for Zero (mV)
on monitor output
with power on, but
pushbutton not pressed yet.
(Controller powered, but
Power Amplifier not
powered.)
Adjust before adjusting
Monitor Gain.

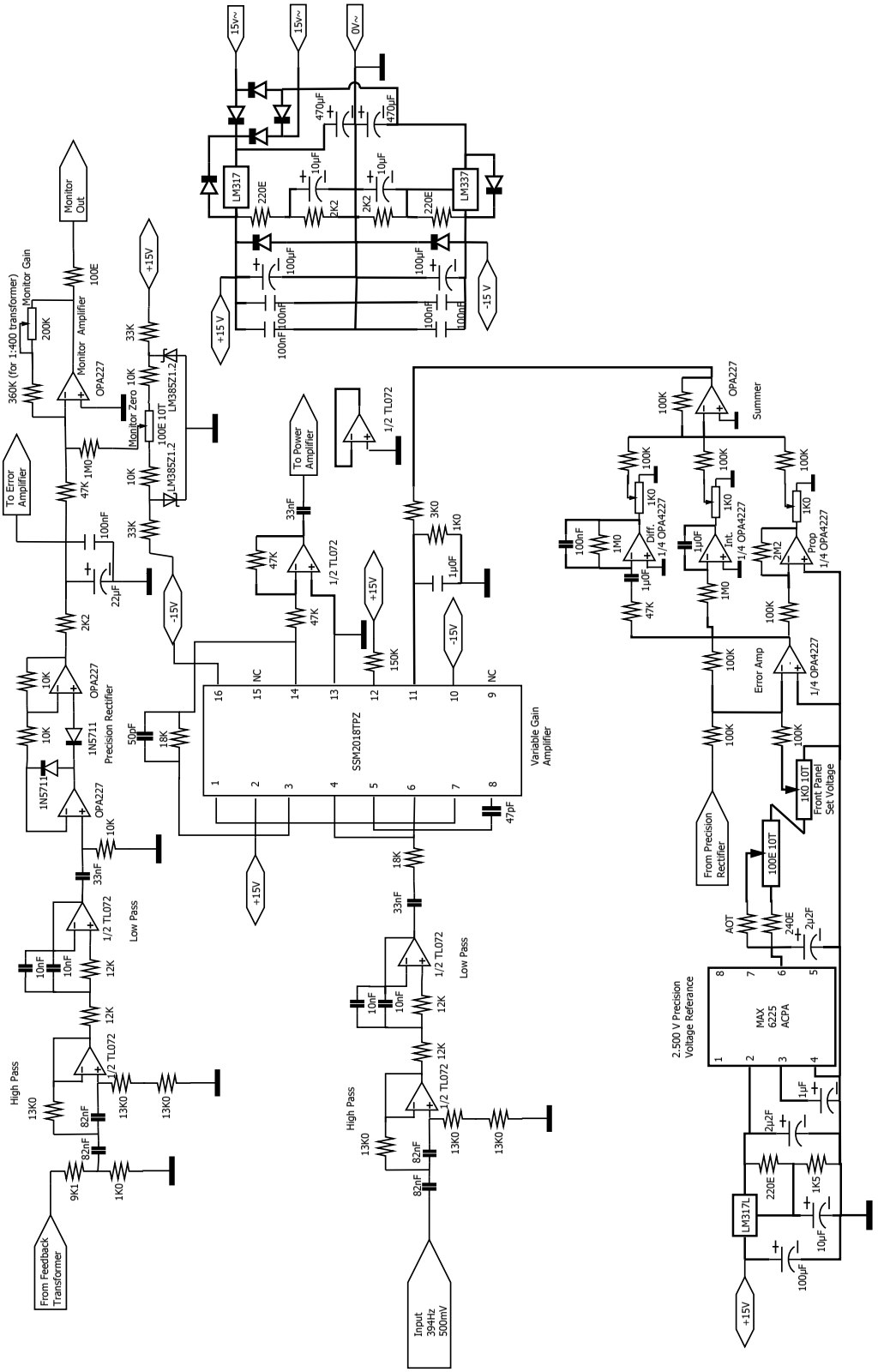
15v~
15v~
0V~
470µF
470µF
LM317
LM337
220E
220E
10µF
10µF
2K2
2K2
100µF
100µF
100nF
100nF
100nF
100nF
+15 V
-15 V
Monitor Out
Monitor Amplifier
OPA227
100E
360K (for 1:400 transformer)
Monitor Gain
200K
Monitor Zero
100E 10T
LM385Z1.2
LM385Z1.2
33K
10K
47K 1M0
10K
33K
100nF
22µF
2K2
To Error Amplifier
+15V
-15V
To Power Amplifier
33nF
47K
47K
1/2 TL072
1/2 TL072
+15V
150K
3K0
1K0
1µ0F
-15V
Variable Gain Amplifier
SSM2018TPZ
NC
NC
50pF
18K
47pF
+15V
10K
10K
1N5711
1N5711
Precision Rectifier
OPA227
OPA227
10K
33nF
1/2 TL072
Low Pass
10nF
10nF
12K
12K
1/2 TL072
High Pass
13K0
82nF
82nF
13K0
13K0
9K1
1K0
From Feedback Transformer
18K
33nF
1/2 TL072
Low Pass
10nF
10nF
12K
12K
1/2 TL072
High Pass
13K0
82nF
82nF
13K0
13K0
Input 394Hz 500mV
OPA227
Summer
100K
100K
100K
100K
1K0
1K0
1K0
100nF
1M0
Diff.
1/4 OPA4227
1µ0F
1µ0F
47K
Int.
1/4 OPA4227
1M0
Prop
1/4 OPA4227
2M2
100K
Error Amp
1/4 OPA4227
100K
100K
From Precision Rectifier
1K0 10T
Front Panel Set Voltage
10E 10T
AOT
240E
2µ2F
2.500 V Precision Voltage Referance
MAX 6225 ACPA
1µF
2µ2F
220E
1K5
LM317L
10µF
100µF
+15V

Appendix B

HPBasic code for calibration of the water Faraday cell

```
10 ! Program to automate calibration of the Water Faraday Cell
20 ! Written by Vincent Couling and Siyabonga Ntombela
30 ! 8 February 2013
40 ! Modified the FCCALIB5.BAS program for the Agilis Controller
50 ! Don't forget to load the 32-bit serial driver: Load Bin "serial32"
60 ! Uses RS232 port to control CONEX-P Agilis precision rotator
controller
70 ! Driving the AG-PR100P rotation stage
80 ! Need a laser, polarizer, glass FC (ac current), water FC (dc
current), analyzer and photodiode detector
90 COM
Ja,Psd(12),Ang(12),Currentzero(12),Psdzero(12),M(30000),C(30000),R(3000
0),T
100 COM Order(12),Jj,Temp
110 Jj=1
120 Order(1)=1
130 Order(2)=10
140 Order(3)=2
150 Order(4)=9
160 Order(5)=3
170 Order(6)=8
180 Order(7)=4
190 Order(8)=7
200 Order(9)=5
210 Order(10)=6
220 ON KEY 6 LABEL "Terminate" GOTO 1920
230 CLEAR SCREEN
240 PRINT "INPUT PSD TIME CONSTANT"
250 INPUT T$
260 PRINT "INPUT PSD SENSITIVITY"
270 INPUT S$
280 Fccalib1$="130213-FCcalib1a"
290 Fccalib2$="130213-FCcalib2a"
300 CREATE Fccalib1$,1
310 CREATE Fccalib2$,1
320 PRINTER IS Fccalib1$;APPEND
330 PRINT "Date is ";DATE$(TIMEDATE)
340 PRINT "Time is ";TIME$(TIMEDATE)
350 PRINT "Automated calibration of the water Faraday Cell ... "
360 PRINT "************************************************"
370 PRINT "     "
380 PRINT "PSD time constant is ",T$
390 PRINT "PSD sensitivity is ",S$
400 PRINTER IS Fccalib2$;APPEND
410 PRINT "Date is ";DATE$(TIMEDATE)
420 PRINT "Time is ";TIME$(TIMEDATE)
430 PRINT "Automated calibration of the water Faraday Cell ... "
440 PRINT "PSD time constant is ",T$
450 PRINT "PSD sensitivity is ",S$
460 PRINT "Calibration constants in microradians per milliamp ... "
470 PRINTER IS CRT
480 ASSIGN @File TO Fccalib1$;APPEND
490 ASSIGN @File TO Fccalib2$;APPEND
500 ASSIGN @Devices TO 1
510 ASSIGN @Io_path TO 9
520 T=0
530 PRINT STATUS(9,3)
540 CONTROL 9,3;57600 ! set the baud rate to 57 600 bps
```

```
550 PRINT STATUS(9,3)
560 PRINT "Start ..."
570 OUTPUT 9;"1VE"
580 PRINT "Check VE version ..."
590 ENTER 9;Ja$
600 WAIT 1
610 PRINT "1VE = ",Ja$
620 PRINT "Finding home ..."
630 OUTPUT 9;"1OR" ! Execute home search
640 PRINT "Wait 30 seconds ..."
650 WAIT 30
660 Prism_min=81.3
670 Prism_max=82.1
680 Prism_min$=VAL$(Prism_min)
690 Prism_max$=VAL$(Prism_max)
700 PRINT "Prism rotating to minimum position of ",Prism_min,"degrees ..."
710 OUTPUT 9;"1PA"&Prism_min$
720 Ang(1)=Prism_min
730 PRINT "Wait 30 seconds ..."
740 WAIT 30
750 OUTPUT 705;"*rst,*cls" ! reset and configure dc power supply
760 OUTPUT 705;"appl p6v, 6.0, 0.0" ! set dc current to zero amps
770 OUTPUT 705;"outp on"
780 OUTPUT 722;"*rst,*cls" ! reset and configure the DMM to read dc current
790 OUTPUT 722;"conf:curr:dc"
800 Currentacc=0 ! set the accumulated current vaiable to zero
810 OUTPUT 709;"*rst" ! reset and configure the Data Acquisition Unit (DAU)
820 OUTPUT 709;"*cls"
830 OUTPUT 709;"rout:scan (@103,106)" ! channel 103 reads the PSD voltage
840 FOR N=1 TO 10 ! determines 10 equally-spaced current settings
850 Cur=Order(N)*.2 ! dc current ranges between 0.2 to 2.0 amps in 0.2 amp
steps, staggered to avoid heating Faraday Cell
860 Cur$=VAL$(Cur) ! numerical value converted to a string
870 Currentacc=0 ! set the accumulated current variable to zero
880 WAIT 1
890 OUTPUT 705;"appl p6v, 6.0, ";Cur$ ! set dc current
900 OUTPUT 705;"outp on"
910 WAIT 5 ! pause for settling
920 FOR Prism=1 TO 10 ! determines 10 equally-spaced prism settings
930 Angle=Prism_min+(Prism_max-Prism_min)*(Prism-1)/9 ! angle to rotate the
prism to
940 Ang(Prism)=Angle
950 OUTPUT 9;"1PA"&VAL$(Angle)
960 PRINTER IS Fccalib1$;APPEND
970 PRINT "Prism Setting = ",Angle," degrees"
980 PRINTER IS CRT
990 PRINT "Prism Setting = ",Angle," degrees"
1000 WAIT 10
1010 OUTPUT 722;"measure:curr:dc?"! measure the dc current
1020 ENTER 722;Ct
1030 Currentacc=Currentacc+Ct! update the accumulated current variable
1040 OUTPUT 709;"conf:volt:dc (@103)"! configure the DAU channel 103 to
read the PSD dc Volts
1050 V=0! current voltage variable
1060 Vtot=0! accumulated voltage variable
```

```
1070 FOR Ii=1 TO 20! accumulate 20 PSD voltage readings
1080 OUTPUT 709;"read?"! read the current voltage
1090 ENTER 709;V
1100 Vtot=Vtot+V! accumulate the voltage readings
1110 WAIT 1/10
1120 NEXT Ii
1130 Vtot=Vtot/20! determine the average PSD voltage for this
current/prism setting
1140 PRINTER IS Fccalib1$;APPEND
1150 PRINT "Vtot ",Prism," = ",Vtot
1160 PRINTER IS CRT
1170 PRINT "Vtot ",Prism," = ",Vtot
1180 Psd(Prism)=Vtot! store the average PSD voltage in an array
1190 NEXT Prism
1200 Currentzero(N)=Currentacc/10
1210 REM linear regression
1220 X=0
1230 Xy=0
1240 Y=0
1250 X2=0
1260 Y2=0
1270 FOR Ij=1 TO 10
1280 Y=Y+Psd(Ij)
1290 X=X+Ang(Ij)
1300 Xy=Xy+Ang(Ij)*Psd(Ij)
1310 X2=X2+Ang(Ij)*Ang(Ij)
1320 Y2=Y2+Psd(Ij)*Psd(Ij)
1330 NEXT Ij
1340 M(N)=(10*Xy-X*Y)/(10*X2-X^2)
1350 C(N)=(Y*X2-X*Xy)/(10*X2-X^2)
1360 R(N)=SQR((10*Xy-X*Y)^2/((10*X2-X^2)*(10*Y2-Y^2)))
1370 PRINTER IS Fccalib1$;APPEND
1380 PRINT "Psd Voltage versus Rotational Angle for a current of
"&Cur$&" Amps"
1390 PRINT "m = ",M(N)
1400 PRINT "c = ",C(N)
1410 PRINT "r = ",R(N)
1420 PRINTER IS CRT
1430 PRINT "Psd Voltage versus Rotational Angle for a current of
"&Cur$&" Amps"
1440 PRINT "m = ",M(N)
1450 PRINT "c = ",C(N)
1460 PRINT "r = ",R(N)
1470 Psdzero(N)=-C(N)/M(N)
1480 WAIT 15
1490 NEXT N
1500 FOR N=1 TO 10
1510 PRINTER IS Fccalib1$;APPEND
1520 PRINT "psdzero ",N,Psdzero(N)," curr ",Currentzero(N)
1530 PRINTER IS CRT
1540 PRINT "psdzero ",N,Psdzero(N)," curr ",Currentzero(N)
1550 NEXT N
1560 X=0
1570 Xy=0
1580 Y=0
1590 X2=0
1600 Y2=0
1610 FOR N=1 TO 10
```

```
1620 Y=Y+Psdzero(N)
1630 X=X+Currentzero(N)
1640 Xy=Xy+Currentzero(N)*Psdzero(N)
1650 X2=X2+Currentzero(N)*Currentzero(N)
1660 Y2=Y2+Psdzero(N)*Psdzero(N)
1670 NEXT N
1680 M(Jj)=(10*Xy-X*Y)/(10*X2-X^2)
1690 C(Jj)=(Y*X2-X*Xy)/(10*X2-X^2)
1700 R(Jj)=SQR((10*Xy-X*Y)^2/((10*X2-X^2)*(10*Y2-Y^2)))
1710 OUTPUT 709;"conf:temp FRTD,85,(@106)" ! measure room temp
1720 OUTPUT 709;"read?"
1730 ENTER 709;Temp
1740 PRINTER IS Fccalib1$;APPEND
1750 PRINT "Plot of Angle for Psd Null versus DC current in Faraday Cell
for run number ",Jj
1760 PRINT "m = ",M(Jj)
1770 PRINT "c = ",C(Jj)
1780 PRINT "r = ",R(Jj)
1790 PRINT "Calibration constant of water Faraday cell is
",M(Jj)*2*3.14159265/360/1000," rad per mA"
1800 PRINT "Temperature of lab is ",Temp," degrees C"
1810 PRINTER IS Fccalib2$;APPEND
1820 PRINT M(Jj)*2*3.14159265/360*1000
1830 PRINTER IS CRT
1840 PRINT "Plot of Angle for Psd Null versus DC current in Faraday Cell
for run number ",Jj
1850 PRINT "m = ",M(Jj)
1860 PRINT "c = ",C(Jj)
1870 PRINT "r = ",R(Jj)
1880 PRINT "Calibration constant of water Faraday cell is
",M(Jj)*2*3.14159265/360/1000," rad per mA"
1890 PRINT "Temperature of lab is ",Temp," degrees C"
1900 Jj=Jj+1
1910 GOTO 840
1920 END
```

Appendix C

HPBasic code for controlling the EFGIB experiment at any temperature

```
10    REM ******************************************************
20    REM Program to control the EFGIB experiment             ****
30    REM Written 08 November 2005 by Naven Chetty            ****
40    REM Modified 02 May 2012 by Couling & Ntombela          ****
50    REM Modified 6 March 2013 by Vincent Couling            ****
60    REM Modified O2SIYAQUAD_1S_316OFFSET_TEMP               ****
70    REM New program initially called EFIGI_O2               ****
80    REM Always set Prism min and max values +/- 0.5 degree  ****
90    REM MODIFIED for 0.5 degree analyzer offset             ****
100   REM Using the AG-PR100P rotation stage and the ...      ****
110   REM ... CONEX-P Agilis precision rotator controller     ****
120   REM ******************************************************
130   COM Ve
140   CLEAR SCREEN
150   REM ********************************************************
160   REM Open communications with the CONEX-P Agilis controller ...
170   REM ... and rotate the prism to home
180   REM ********************************************************
190   ASSIGN @Devices TO 1
200   ASSIGN @Io_path TO 9
210   CONTROL 9,3;57600 ! set the BAUD rate to 57 000 bps
220   OUTPUT 9;"1VE"
230   PRINT "Check VE version ... "
240   ENTER 9;Ve$
250   WAIT 1
260   PRINT "1VE = ";Ve$
270   PRINT "Finding home ... "
280   OUTPUT 9;"1OR" ! Execute home search
290   PRINT "Wait 30 seconds ... "
300   WAIT 3
310   REM **************************
320   REM File names for data storage
330   REM **************************
340   Efgibfile1$="14Mar2013-1efgib"
350   Tempfile1$="14Mar2013-1temp"
360   Currentfile1$="14Mar2013-1curr"
370   Datafile1$="14Mar2013-1data"
380   PRINTER IS CRT ! The variables are declared in statements below.
390   REM ************************
400   REM declare common variables
410   REM ************************
420   COM
I,Counter1,No1,Sig1,T,Temp45(1000),Preset(1000),Pg,Pa,Psd(25),Iac(25),Hvac(
25)
430   COM
Hv(15),M(1000),C(1000),R(1000),Nulli(1000),Hiv(1000),Ctime(3200),Counting
431   COM M_2(1000),C_2(1000),R_2(1000),Nulli_2(1000)
440   COM Switch(3200),W,V,Counterp1,Counterp2,Diff,Err45,Err4tsp,Pid_dl
450   COM
Acumsec2(3200),Ferrlast,Ferr1,Time3,Time4,Time5,Difftime,Counter2,Vtot
460   COM Efgibfile$[40],Tempfile$[40],Presfile$[40],Warning$[80]
470   COM
Highvolts,Ni,Err1(3200),Err2(3200),Err3(3200),Err4(3200),Temperature
480   COM
Err5(3200),C02,Int1(3200),Closetime(3200),Scaledtime,Voltage1,Voltage2,Temp
45a(1000)
490   COM Temp45b(1000),Temp45c(1000),Param,Volta,Voltb,Zz(1000)
500   COM Param1,Param2,Param3!,Param4
510   COM Prism_min,Prism_max,Res,Iac_2(25)
511   !COM Prism_min1$,Prism_max1$
520   Scaledtime=0
```

```
530   Ni=1
540   REM
************************************************************************
550   REM Establish the analyzer offsets using CONEX.BAS, then modify
accordingly ...
560   REM ... for the max and min limits below:
570   REM
************************************************************************
580   Prism_min=80.9 ! These two values should differ by 1 degree
581   PRINT "Prism min ";Prism_min
590   Prism_max=81.9 ! so that the offset is +/- 0.5 of a degree
591   PRINT "Prism max ";Prism_max
600   Prism_min$="80.9" ! converts the value to a string
610   Prism_max$="81.9"
620   PRINT "Prism rotating to maximum position of ",Prism_max," degrees ... "
630   OUTPUT 9;"1PA"&Prism_max$
640   PRINT "Wait 30 seconds ... "
650   WAIT 30
660   REM ******************************
670   REM Open the files for data storage
680   REM ******************************
690   CREATE Efgibfile1$,1
700   CREATE Tempfile1$,1
710   CREATE Currentfile1$,1
720   CREATE Datafile1$,1
730   ASSIGN @File TO Efgibfile1$;APPEND
740   ASSIGN @File TO Tempfile1$;APPEND
750   ASSIGN @File TO Currentfile1$;APPEND
760   ASSIGN @File TO Datafile1$;APPEND
770   PRINT "Please enter gas name" !User inputs the name of the gas.
780   INPUT Gasname$
790   PRINT "please enter gas pressure (MPa)" !User inputs the pressure.
800   INPUT Pg
810   PRINT "please enter PSD time constant" ! ususally 1 sec
820   INPUT Param$
830   PRINT "please enter PSD sensitivity" ! ? micro Volts
840   INPUT Param1$
850   PRINT "please enter type of Faraday Cell" ! Water, toluene, glass?
860   INPUT Param2$
870   PRINT "please enter Faraday Cell current-limiting resistance" ! to limit
the Faraday Cell current
880   INPUT Param3$
885   Res=2614.9 ! The 4-wire R value to confirm the ac Faraday Cell current
890   CLEAR SCREEN
900   PRINTER IS Efgibfile1$;APPEND
910   PRINT "Measurement of molecular quadrupole moment for ";Gasname$
920   PRINT "Time is ";TIME$(TIMEDATE)
930   PRINT "Date is ";DATE$(TIMEDATE)
940   PRINT "Cell pressure (gauge) in  MPa ";Pg
950   PRINT "PSD time constant  ";Param$
960   PRINT "PSD sensitivity  ";Param1$
970   PRINT "Type of Faraday Cell  ";Param2$
980   PRINT "Faraday Cell current-limiting resistance  ";Param3$
990   PRINT "Maximum analyzer offset is (degrees)  ";Prism_max
1000  PRINT "Minimum analyzer offset is (degrees)  ";Prism_min
1010  PRINTER IS CRT
1020  Counter1=1
1030  No1=0
1040  Sig1=1
1050  ON KEY 6 LABEL "Terminate" GOTO 3060
```

```
1060  REM ********************************
1070  REM reset and initialize Agilent DAU
1080  REM ********************************
1090  OUTPUT 709;"*rst"       !Reset data acquisition unit to factory
settings.
1100  OUTPUT 709;"*cls"
1110  PRINT "SWITCH ON HV, AND PRESS ENTER"
1120  ON KBD GOTO 1130
1130  OUTPUT 709;"rout:scan(@101,102,103,104,105,106,112,122)"
1140  CLEAR SCREEN
1150  PRINTER IS Efgibfile1$;APPEND
1160  Highvolts=0
1170 Counting=0
1180   OUTPUT 709;"route:close (@201)"  !Reset the current attenuator to
zero
1190   OUTPUT 709;"route:open (@201)"
1200  OUTPUT 709;"route:close (@203)"   !Transfer to reset counter to zero
1210  OUTPUT 709;"route:close (@203)"
1220 Temperature=0
1230  FOR Z=0 TO 9 !Do loop for taking 10 measurments.
1240   FOR I=0 TO 50  !Do loop to vary current through FC and change phase.
1250   OUTPUT 709;"route:close (@202)"  !count 50 time then change current
ic FC
1260   OUTPUT 709;"route:open (@202)"
1270  !Counting=Counting+I
1280   NEXT I
1290  !PRINT "i = ",I
1300  Counting=Counting+I
1310  !PRINT "Counting = ",Counting
1320  OUTPUT 709;"route:close (@203)" !Data transfer occurs at this point.
1330  OUTPUT 709;"route:close (@203)"
1340  WAIT 5
1350  OUTPUT 709;"conf:curr:ac (@122)"  !Read the current in FC
1360  OUTPUT 709;"read?"
1370  ENTER 709;Iac(Z+1)
1371  OUTPUT 709;"conf:volt:ac (@112)"  !Read the voltage across the FC
resistor
1372  OUTPUT 709;"read?"
1373  ENTER 709;Iac_2(Z+1)
1374  Iac_2(Z+1)=Iac_2(Z+1)/Res
1380 IF Counting>256 THEN Iac(Z+1)=-1*Iac(Z+1) !Manually change current
phase
1382 IF Counting>256 THEN Iac_2(Z+1)=-1*Iac_2(Z+1) !Manually change current
phase
1390  PRINTER IS CRT
1400  !WAIT 5
1410  OUTPUT 709;"conf:temp TC,J,(@101)" !Measure the room temperature
using a J-type thermocouple
1420  OUTPUT 709;"read?"
1430  OUTPUT 709;"read?"
1440  ENTER 709;Temp45(Z+1)
1450  OUTPUT 709;"conf:temp FRTD,85,(@105)" !Measure the cell temperature
using a PT100, 4-wire
1460  OUTPUT 709;"read?"
1470  ENTER 709;Temp45a(Z+1)
1480  !Temp45a(Z+1)=Temp45(Z+1)
1490  OUTPUT 709;"conf:temp FRTD,85,(@106)" !Measure the cell temperature
using a PT100
1500  OUTPUT 709;"read?"
1510  ENTER 709;Temp45b(Z+1)
1520  !Temp45b(Z+1)=Temp45(Z+1)
```

```
1530  OUTPUT 709;"conf:temp FRTD,85,(@107)" !Measure the cell temperature
using a PT100
1540  OUTPUT 709;"read?"
1550  ENTER 709;Temp45c(Z+1)
1560  !Temp45c(Z+1)=Temp45(Z+1)
1570  !WAIT 6
1580  GOSUB 1970 !Take 20 psd reading and average
1590  !OUTPUT 709;"conf:volt:dc (@103)" !Measure psd voltages
1600  !OUTPUT 709;"read?"
1610  !ENTER 709;Psd(Z+1)
1620  PRINTER IS Efgibfile1$;APPEND
1630  !PRINT "Voltage =";Psd(Z+1);"Current is ";Iac(Z+1) !Measure current
in FC.
1640  OUTPUT 709;"conf:volt:dc (@104)"
1650  OUTPUT 709;"read?"
1660  ENTER 709;Hvac(Z+1)
1670  Highvolts=Highvolts+Hvac(Z+1)
1680  Temperature=Temperature+(Temp45a(Z+1)+Temp45b(Z+1)+Temp45c(Z+1))/3
1690  PRINT "Voltage = ";Psd(Z+1);"Current is ";Iac(Z+1),"Hv is
";Hvac(Z+1);Counting;Temp45a(Z+1);Temp45b(Z+1);Temp45c(Z+1)
1691  PRINT "Voltage = ";Psd(Z+1);"C_2 is ";Iac_2(Z+1),"Hv is
";Hvac(Z+1);Counting;Temp45a(Z+1);Temp45b(Z+1);Temp45c(Z+1)
1700  PRINTER IS CRT ! _2 is FC measured via V and R
1710  PRINT "Voltage = ";Psd(Z+1);"Current is ";Iac(Z+1),"Hv is
";Hvac(Z+1);Counting;Temp45a(Z+1);Temp45b(Z+1);Temp45c(Z+1)
1711  PRINT "Voltage = ";Psd(Z+1);"C_2 is ";Iac_2(Z+1),"Hv is
";Hvac(Z+1);Counting;Temp45a(Z+1);Temp45b(Z+1);Temp45c(Z+1)
1720  NEXT Z
1730  PRINT "the average high voltage to the cell is ";Highvolts/10
1740  GOSUB 2120  !perform linear regression after each run
1750  PRINTER IS Efgibfile1$;APPEND
1760  Ni=Ni*(-1)
1770  REM
*************************************************************************
****
1780  REM Subroutine used to rotate stepper motor and hence the analyser to
desired value.
1790  REM
*************************************************************************
****
1800  IF Ni=1 THEN GOTO 1820
1810  IF Ni=-1 THEN GOTO 1860
1820  OUTPUT 9;"1PA"&Prism_max$
1830  WAIT 15
1840  PRINT "rotated forward ... "
1850  GOTO 1140
1860  OUTPUT 9;"1PA"&Prism_min$
1870  WAIT 15
1880  PRINT "rotated backwards ... "
1890  GOTO 1140
1900  REM **************************
1910  REM **************************
1920  PRINT "end"
1930  PRINT "end"
1940  !GOTO 4100 !Compute mQ
1950  REM
1960  REM
1970  REM ***************************************************************
1980  REM The subroutine to take 20 psd readings and calculate it average
1990  REM ***************************************************************
2000  OUTPUT 709;"conf:volt:dc (@103)" !Measure psd voltages
```

```
2010  Voltage1=0
2020  Voltage2=0
2030  WAIT 5
2040  FOR Ii=1 TO 20
2050  OUTPUT 709;"read?"
2060  ENTER 709;Voltage1
2070  Voltage2=Voltage2+Voltage1
2080  WAIT 1/2
2090  NEXT Ii
2100  Psd(Z+1)=Voltage2/20
2110  RETURN
2120  REM ******************************************
2130  REM The subroutine to perform linear regression
2140  REM ******************************************
2150  REM
2160  No1=No1+1
2170  X=0
2171  X_2=0
2180  Xy=0
2181  Xy_2=0
2190  Y=0
2200  X2=0
2201  X2_2=0
2210  Y2=0
2220  Zz(No1)=Psd(10)
2230  FOR Ij=1 TO 10
2240  Y=Y+Psd(Ij)
2250  X=X+Iac(Ij)
2251  X_2=X_2+Iac_2(Ij)
2260  Xy=Xy+Iac(Ij)*Psd(Ij)
2261  Xy_2=Xy_2+Iac_2(Ij)*Psd(Ij)
2270  X2=X2+Iac(Ij)*Iac(Ij)
2271  X2_2=X2_2+Iac_2(Ij)*Iac_2(Ij)
2280  Y2=Y2+Psd(Ij)*Psd(Ij)
2290  NEXT Ij
2300  M(No1)=(10*Xy-X*Y)/(10*X2-X^2)
2301  M_2(No1)=(10*Xy_2-X_2*Y)/(10*X2_2-X_2^2)
2310  C(No1)=(Y*X2-X*Xy)/(10*X2-X^2)
2311  C_2(No1)=(Y*X2_2-X_2*Xy_2)/(10*X2_2-X_2^2)
2320  R(No1)=SQR((10*Xy-X*Y)^2/((10*X2-X^2)*(10*Y2-Y^2)))
2321  R_2(No1)=SQR((10*Xy_2-X_2*Y)^2/((10*X2_2-X_2^2)*(10*Y2-Y^2)))
2330  Hiv(No1)=Highvolts/10
2340  PRINTER IS Efgibfile1$;APPEND
2350  PRINT
2360  PRINT "slope = ";M(No1)/1000;"V/mA"
2361  PRINT "slope_2 = ";M_2(No1)/1000;"V/mA"
2370  PRINT "intercept = ";C(No1);"v"
2371  PRINT "intercept_2 = ";C_2(No1);"v"
2380  PRINT "r = ";R(No1)
2381  PRINT "r_2 = ";R_2(No1)
2390  PRINT "Zz(1) = ";Zz(1)
2400  PRINT
2410  PRINT
2420  PRINTER IS CRT
2430  PRINT "slope = ",M(No1)/1000;"v/mA"
2431  PRINT "slope_2 = ",M_2(No1)/1000;"v/mA"
2440  PRINT "intercept = ";C(No1);"V"
2441  PRINT "intercept_2 = ";C_2(No1);"V"
2450  PRINT "r = ";R(No1)
2451  PRINT "r_2 = ";R_2(No1)
2460  PRINT "Zz(1) = ";Zz(1)
```

```
2470  PRINT
2480  IF R(No1)<.995 THEN
2490  IF No1 MOD 2 THEN
2500  R(No1)=R(No1-1)
2501  R_2(No1)=R_2(No1-1)
2510  END IF
2520  No1=No1-1
2530  PRINT "bad run"
2540  GOTO 1160
2550  END IF
2560  IF Sig1=-1 THEN GOSUB 2600
2570  Sig1=-1*Sig1
2580  RETURN
2590  REM
2600  REM ******************************************
2610  REM The subroutine to determine the null current
2620  REM ******************************************
2630  REM
2640  Nulli(No1/2)=(C(No1)-C(No1-1))/(M(No1-1)-M(No1))
2641  Nulli_2(No1/2)=(C_2(No1)-C_2(No1-1))/(M_2(No1-1)-M_2(No1))
2650  Nullpsd=M(No1)*Nulli(No1/2)+C(No1)
2651  Nullpsd_2=M_2(No1)*Nulli_2(No1/2)+C_2(No1)
2660  PRINTER IS Efgibfile1$;APPEND
2670  PRINT
2680  PRINT "Run no ";No1/2
2690  PRINT "the null current is ";Nulli(No1/2)*1000;"mA"
2691  PRINT "the null current_2 is ";Nulli_2(No1/2)*1000;"mA"
2700  PRINT "the null voltage is ";Nullpsd;"V"
2701  PRINT "the null voltage_2 is ";Nullpsd_2;"V"
2710  PRINT " the correlation co-efficients were ";R(No1-1);" and";R(No1)
2711  PRINT " the correlation co-efficients_2 were ";R_2(No1-1);"
and";R_2(No1)
2720  Temp45(No1/2)=FNTemperature
2730  PRINT Counter1;"room temp";Temperature/10;"pressure ";Pg;"time =
";TIME$(TIMEDATE);"date";DATE$(TIMEDATE)
2740 PRINT "High voltage average ",Highvolts/10
2750  PRINT
2760  PRINT
2770  PRINTER IS Datafile1$;APPEND
2780  PRINT "Run no ";No1/2
2790  PRINT "the null current is ";Nulli(No1/2)*1000;"mA"
2791  PRINT "the null current_2 is ";Nulli_2(No1/2)*1000;"mA"
2800  PRINT "the null voltage is ";Nullpsd;"V"
2801  PRINT "the null voltage_2 is ";Nullpsd_2;"V"
2810  PRINT " the correlation co-efficients were ";R(No1-1);" and";R(No1)
2811  PRINT " the correlation co-efficients_2 were ";R_2(No1-1);"
and";R_2(No1)
2820  PRINT "slope = ",M(No1)/1000;"v/mA"
2821  PRINT "slope_2 = ",M_2(No1)/1000;"v/mA"
2830  PRINT "intercept = ";C(No1);"V"
2831  PRINT "intercept_2 = ";C_2(No1);"V"
2840  !PRINTER IS CRT
2850  !Pres(No1/2)=Pg
2860  PRINT
2870  PRINT
2880  PRINTER IS CRT
2890  PRINT "Run no ";No1/2
2900  PRINT "the null current is ";Nulli(No1/2)*1000;"mA"
2901  PRINT "the null current_2 is ";Nulli_2(No1/2)*1000;"mA"
2910  PRINT "the null voltage is ";Nullpsd;"V"
2911  PRINT "the null voltage_2 is ";Nullpsd_2;"V"
```

```
2920  PRINT " the correlation co-efficients were ";R(No1-1);" and";R(No1)
2921  PRINT " the correlation co-efficients_2 were ";R_2(No1-1);"
and";R_2(No1)
2930  PRINT Counter1;"room temp";Temperature/10;"pressure ";Pg;"time =
";TIME$(TIMEDATE);"date = ";DATE$(TIMEDATE)
2940  PRINTER IS Currentfile1$;APPEND
2950  PRINT
Nulli(No1/2)*1000;Nulli_2(No1/2)*1000;Temperature/10;Highvolts/10
2960  PRINTER IS Tempfile1$;APPEND
2970  PRINT "Run no ";No1/2
2980  PRINT "the null current is ";Nulli(No1/2)*1000;"mA"
2981  PRINT "the null current_2 is ";Nulli_2(No1/2)*1000;"mA"
2990  PRINT "the null voltage is ";Nullpsd;"V"
2991  PRINT "the null voltage_2 is ";Nullpsd_2;"V"
3000  PRINT " the correlation co-efficients were ";R(No1-1);" and";R(No1)
3001  PRINT " the correlation co-efficients_2 were ";R_2(No1-1);"
and";R_2(No1)
3010  PRINT Counter1;"cell temp";Temperature/10;"pressure ";Pg;"time =
";TIME$(TIMEDATE);"date= ";DATE$(TIMEDATE)
3020  PRINT "High voltage average ",Highvolts/10
3030  PRINT
3040  PRINT
3050  RETURN
3060  END
3070  REM ************************************************
3080  REM The subfunction to determine the room temperature
3090  REM ************************************************
3100  DEF FNTemperature
3110  OUTPUT 709;"conf:temp TC,J,(@101)"
3120  OUTPUT 709;"read?"
3130  ENTER 709;Temp4
3140  RETURN Temp45
3150  Volta=Voltage1
3160  FNEND
```

Appendix D

Peer-reviewed Publication

Chemical Physics Letters 614 (2014) 41–44

Contents lists available at ScienceDirect

Chemical Physics Letters

journal homepage: www.elsevier.com/locate/cplett

The electric quadrupole moment of O_2

Vincent W. Couling*, Siyabonga S. Ntombela

School of Chemistry and Physics, University of KwaZulu-Natal, Private Bag X01, Scottsville, 3209 Pietermaritzburg, South Africa

ARTICLE INFO

Article history:
Received 10 July 2014
In final form 3 September 2014
Available online 10 September 2014

ABSTRACT

Room-temperature measurements of the Buckingham effect (electric-field-gradient-induced birefringence, EFGIB) for gaseous oxygen are presented. The traceless electric quadrupole moment of the oxygen molecule has been deduced from these data, with the assumption that the temperature-independent hyperpolarizability contribution to the EFGIB is negligibly small. The value obtained is $\Theta = (-1.033 \pm 0.027) \times 10^{-40}$ C m^2. This value is compared with the best available *ab initio* quantum computational values in the literature.

1. Introduction

The molecular quadrupole moment Θ of O_2 has recently been calculated by Bartolomei et al. using high-level multiconfigurational *ab initio* methods [1]. The attainment of high accuracy in *ab initio* computations of molecular properties such as Θ is a non-trivial task, requiring the use of large basis sets and the inclusion of electron correlation [1,2]. Accurate experimental values for these molecular properties can serve as useful benchmarks against which to assess the effects arising from the application of higher levels of *ab initio* theory. Unfortunately, there is currently a paucity of experimental data of Θ for O_2 against which to compare calculated values.

For non-dipolar molecules like O_2, Θ is the leading electric moment describing the molecular charge-distribution and its interaction with external non-uniform electric fields, and so is crucial in describing a range of physical phenomena, including aspects of atmospheric chemical physics, as described in [1,3] and the references therein. The preferred experimental method for measuring Θ of gaseous non-dipolar species is the Buckingham effect (electric-field-gradient-induced birefringence, EFGIB) [4,5]. Our laboratory has yielded recent EFGIB measurements of Θ for CO_2, as well as for the dipolar molecules OCS, N_2O and CO [6–8]. Where possible, temperature-dependent studies are preferred, since this allows for separation of the electronic distortion and molecular orientation contributions to the measured birefringence.

We present here our value of Θ for O_2, which has been obtained from room-temperature EFGIB measurements using the assumption that the electronic distortion contribution to the EFGIB is negligible. Attempts to measure the EFGIB at higher temperatures were unsuccessful, the size of the measured birefringence being particularly small for this species, leading to considerable experimental challenges which we have as yet been unable to overcome.

Coriani and co-workers [9,10] have demonstrated how recent advances in *ab initio* methods have allowed for high accuracy in the computation of first-order molecular properties, allowing them to compute the electronic distortion contribution to the EFGIB for N_2, and thus to perform a correction on the existing room-temperature EFGIB measurements for this molecule, yielding a refined experimental quadrupole moment which was in good agreement with their *ab initio* calculated Θ. A subsequent temperature-dependent experimental study of the Buckingham effect for N_2 essentially confirmed the validity of their analysis [11]. In principle, the measured value of Θ for O_2 presented in this work could be further refined in this manner, with the *ab initio* computation of the electronic distortion contribution to the EFGIB allowing for a similar correction. This task is left to the quantum chemists who are equipped to undertake such a study.

2. Theory

The EFGIB is the anisotropy in the refractive index, $n_x - n_y$, which is observed when light propagates through a fluid along the z-direction, which is perpendicular to an applied electric field gradient $E_{xx} = -E_{yy}$. The molar field-gradient birefringence constant ${}_mQ$ is defined in terms of macroscopic observables as [12]

$$ {}_mQ = \frac{6n(3\epsilon_r + 2)}{5\epsilon_r(n^2+2)^2} \lim_{E_{xx}\to 0} \left(\frac{n_x - n_y}{E_{xx}}\right) V_m, \tag{1} $$

* Corresponding author.
E-mail address: couling@ukzn.ac.za (V.W. Couling).

http://dx.doi.org/10.1016/j.cplett.2014.09.006
0009-2614/

where n and ϵ_r are the refractive index and relative permittivity of the gas in the absence of the field gradient, and V_m is the molar volume of the fluid.

For an axially symmetric non-dipolar molecule like oxygen, making use of the classical equation for the induced birefringence expressed in terms of fundamental molecular properties [13] yields

$$ {}_mQ = \frac{2N_A}{45\epsilon_0}\left[\frac{15}{2}\,b + \frac{\Theta\Delta\alpha}{kT}\right]. \tag{2}$$

Here the hyperpolarizability term b, which is a function of the frequency ω of the incident light, is the grouping of molecular hyperpolarizabilities [13,14]

$$ b = \frac{2}{15}\left(B_{\alpha\beta,\alpha\beta} - \mathcal{B}_{\alpha,\alpha\beta,\beta}\right) - \frac{2}{3\omega}\,\epsilon_{\alpha\beta\gamma}J'_{\alpha,\beta,\gamma}, \tag{3}$$

where $\epsilon_{\alpha\beta\gamma}$ is the Levi-Civita tensor, and the hyperpolarizability tensors $B_{\alpha\beta,\alpha\beta}$, $\mathcal{B}_{\alpha,\alpha\beta,\beta}$ and $J'_{\alpha,\beta,\gamma}$ are defined elsewhere [13]. $\Delta\alpha$ is the optical-frequency dipole polarizability anisotropy, and Θ is the electric quadrupole moment which is defined by

$$ \Theta = \Theta_{33} = -2\Theta_{11} = -2\Theta_{22}, \tag{4}$$

these being the components of the traceless quadrupole moment

$$ \Theta_{\alpha\beta} = \frac{1}{2}\sum_i q_i\left(3r_{i\alpha}r_{i\beta} - r_i^2\delta_{\alpha\beta}\right) \tag{5}$$

where $\mathbf{r}_i$ is the displacement of charge q_i. (Note that unspecified symbols in Eq. (2) and in what follows are taken to refer to fundamental constants in their standard IUPAC notation.)

In the derivation of Eq. (2), the rotational motion of the molecules has been assumed to be classical. For the lighter molecules, such as oxygen, it becomes necessary to consider the effects of the quantization of rotation on the alignment of the molecules in the applied field gradient, as demonstrated by Buckingham and Pariseau [15]. Eq. (2) then becomes

$$ {}_mQ = \frac{2N_A}{45\epsilon_0}\left[\frac{15}{2}\,b' + \frac{\Theta\Delta\alpha}{kT}f(T)\right] \tag{6}$$

where for an axially symmetric molecule with principal moment of inertia I,

$$ f(T) = 1 - \left(\frac{\hbar^2}{2kTI}\right) + \frac{8}{15}\left(\frac{\hbar^2}{2kTI}\right)^2 + \cdots. \tag{7}$$

Note that b' differs slightly from b due to centrifugal distortion. While $f(T)$ for all but the lightest of molecules is close enough to 1, so that quantum corrections can be ignored (e.g. for carbon dioxide at room temperature $f(T) = 0.998$), for oxygen $f(T)$ is 0.9931 at 300 K, and although this correction of 0.7% is small, it is not insignificant, and needs to be taken into account.

3. Experiment and results

The apparatus and experimental techniques used in the measurements of the room-temperature EFGIB of O_2 reported here have been described in detail elsewhere [6]. Measurements of ${}_mQ$ were taken using ultra-high-purity O_2, with a quoted 99.998% minimum purity, supplied by Afrox. The second and third pressure virial coefficients which are required in the calculation of the molar volumes of the gas samples were obtained from the tabulations of Dymond et al. [16]. Refractive indices were calculated from Landolt–Börnstein tables [17] using these molar volumes. The dielectric constant ε_r was calculated using the correlation

$$ \frac{\varepsilon_r - 1}{\varepsilon_r + 2} = A_{\varepsilon,273\,\mathrm{K}}\,\rho\left(1 + b_\varepsilon\rho + c_\varepsilon\rho^2\right) + A_\tau\,\rho\left(\frac{T}{273.16\,\mathrm{K}} - 1\right) \tag{8}$$

as deduced by Schmidt and Moldover [18], where ρ is the molar density. Here, the term with the parameter A_τ accounts for the small temperature dependence of A_ε arising from centrifugal stretching in diatomic molecules. The parameters which we have used in Eq. (8) are taken from recent high-precision ε_r measurements of O_2 at 273 K, 293 K and 323 K, namely $A_{\varepsilon,273\mathrm{K}} = 3.95760\ \mathrm{cm^3\,mol^{-1}}$, $b_\varepsilon = 0.16\ \mathrm{cm^3\,mol^{-1}}$, $c_\varepsilon = -50\ \mathrm{cm^6\,mol^{-2}}$, and $A_\tau = 0.0037\ \mathrm{cm^3\,mol^{-1}}$ [19].

The polarizability anisotropy of $\Delta\alpha = 1.223\times10^{-40}\ \mathrm{C^2\,m^2\,J^{-1}}$ used here was obtained by Bridge and Buckingham from measurements of the low-density depolarization ratio ρ_0 of Rayleigh-scattered light performed at the wavelength 632.8 nm [20]. To estimate the uncertainty in $\Delta\alpha$, the classical expression

$$ \rho_0 = \frac{3(\Delta\alpha)^2}{45\alpha^2 + 4(\Delta\alpha)^2} \tag{9}$$

which relates ρ_0 to $\Delta\alpha$ and the mean dynamic polarizability α can be conveniently recast as

$$ \Delta\alpha = 3\alpha\sqrt{\frac{5\rho_0}{3 - 4\rho_0}}. \tag{10}$$

Bridge and Buckingham obtained $100\rho_0 = (3.02 \pm 0.01)$ for O_2, and estimated an uncertainty of 0.5% for the $\alpha = 1.778\times10^{-40}\ \mathrm{C^2\,m^2\,J^{-1}}$ which they used in their analysis, so that their $\Delta\alpha$ deduced via Eq. (10) would have an uncertainty of 0.7%. The high-precision $\alpha = (1.7803 \pm 0.0003)\times10^{-40}\ \mathrm{C^2\,m^2\,J^{-1}}$ recently measured for O_2 at 632.99 nm by Hohm [21] lies within 0.13% of the value used by Bridge and Buckingham, improving the uncertainty of this component of Eq. (10). Unfortunately, the only other depolarization ratio measured for O_2 at 632.8 nm, namely the $100\rho_0 = (2.9 \pm 0.1)$ obtained by Baas and van den Hout [22], is some 4.2% smaller than Bridge and Buckingham's value. As Bogaard et al. have argued [23], while the precision of a set of ρ_0 values measured by a given investigator can be as high as 0.5% or better, the determinations of different investigators can be discrepant by as much as 4%, so that the accuracy of depolarization ratios is assumed to be no better than $\approx\pm3\%$. The uncertainty in the $\Delta\alpha$ of Bridge and Buckingham is consequently estimated to be around 2.3%, arising from 0.2% in α, and 2.1% in $\sqrt{5\rho_0/(3-4\rho_0)}$ (as compared with the Baas and van den Hout measurement). It should be noted that the *ab initio* calculated $\Delta\alpha = 1.184\times10^{-40}\ \mathrm{C^2\,m^2\,J^{-1}}$ at 632.8 nm of Jonsson et al. [24] lies closer to the $\Delta\alpha = 1.19\times10^{-40}\ \mathrm{C^2\,m^2\,J^{-1}}$ obtained by Baas and van den Hout. This MCSCF computation includes zero-point vibrational averaging. The Bridge and Buckingham $\Delta\alpha$ has been used in the extraction of Θ from Eq. (6) since their depolarization ratio has a statistical uncertainty an order of magnitude smaller than that of Baas and van den Hout, indicating a greater precision of measurement. However, there remains ambiguity as to which of the two ρ_0 values is the more accurate, and so the Baas and van den Hout $\Delta\alpha$ is used to calculate a Θ for comparative purposes. It would appear that fresh light-scattering measurements of O_2 are warranted to bring resolution to this ambiguity.

Several experimental runs were performed at room temperature, and the ${}_mQ$ value for each run, together with the deduced quadrupole moment Θ (assuming $b' = 0$), are presented in Table 1. The uncertainties provided in Table 1 are the standard deviations associated with the measured quantities. The possible sources of systematic error in the measured quantities have been reported in the Letter by Chetty and Couling [6], and arise from the determination of the absolute temperature of the gas (0.2%), the molar volume of the gas (0.3%), the length of the wires in the cell (0.1%), the on-axis electric field gradient (0.4%), and the calibration constant of the Faraday nulling cell (now reduced to 0.2%). The uncertainty in the polarizability anisotropy used in the analysis (2.3%) must also be

Table 1
The Buckingham constant ($_mQ$) values and electric quadrupole moments (Θ) for molecular oxygen measured at room temperature and at a wavelength of 632.8 nm.

$\bar{T}$ (K)	P (MPa)	$10^4 V_m$ ($m^3\,mol^{-1}$)	ε_r	$10^6(n-1)$	$10^{26}{}_mQ$ ($C\,m^5J^{-1}mol^{-1}$)	$10^{40}\Theta$[a] ($C\,m^2$)
298.7	2.715	8.996	1.0133	6675	-0.939 ± 0.034	-1.047 ± 0.070
298.6	2.710	9.011	1.0132	6664	-0.920 ± 0.026	-1.026 ± 0.060
298.3	2.705	9.016	1.0132	6660	-0.930 ± 0.029	-1.036 ± 0.064
298.5	2.702	9.037	1.0132	6645	-0.939 ± 0.028	-1.047 ± 0.063
298.4	2.696	9.053	1.0132	6633	-0.908 ± 0.030	-1.012 ± 0.064
298.2	2.693	9.056	1.0132	6631	-0.910 ± 0.026	-1.021 ± 0.060
298.2	2.681	9.095	1.0131	6602	-0.936 ± 0.022	-1.042 ± 0.056
297.9	2.668	9.133	1.0131	6575	-0.934 ± 0.033	-1.039 ± 0.068
298.2	2.663	9.159	1.0130	6557	-0.937 ± 0.026	-1.044 ± 0.061
297.8	2.653	9.182	1.0130	6540	-0.920 ± 0.031	-1.023 ± 0.066
298.6[b]	2.708	9.043	1.0132	6640	-0.929 ± 0.064	-1.038 ± 0.103
300.2[b]	2.723	9.018	1.0132	6659	-0.920 ± 0.044	-1.031 ± 0.081
300.2[b]	2.722	9.021	1.0132	6657	-0.912 ± 0.082	-1.022 ± 0.123
300.5[b]	2.724	9.031	1.0132	6649	-0.929 ± 0.058	-1.038 ± 0.096
300.6[b]	2.720	9.041	1.0132	6642	-0.921 ± 0.064	-1.034 ± 0.103

[a] Computed using $f(\bar{T}) = 0.9931$ in Eq. (6).
[b] These data were measured after a complete reassembling and realignment of the quadrupole cell, including assembly of a new set of wire electrodes.

taken into account. The final uncertainty ascribed to the deduced mean Θ is a combination of maximum errors and standard deviations, as proposed by Baird [25], this final uncertainty denoting an interval over which the probability of finding the true quadrupole moment is estimated to be two-thirds.

The first 10 measurements in Table 1 yield a quadrupole moment of $\Theta = (-1.034 \pm 0.027) \times 10^{-40}\,C\,m^2$, while the last five measurements (see Table 1, footnote b), which were recorded after the quadrupole cell was completely dismantled and reassembled with a new set of wire electrodes, is $\Theta = (-1.033 \pm 0.027) \times 10^{-40}\,C\,m^2$. The combined 15 measurements yield a quadrupole moment of $\Theta = (-1.033 \pm 0.027) \times 10^{-40}\,C\,m^2$.

If the $\Delta\alpha$ of Baas and van den Hout (together with its uncertainty quoted in [22]) is used instead of that of Bridge and Buckingham, the combined 15 measurements yield a quadrupole moment of $\Theta = (-1.062 \pm 0.042) \times 10^{-40}\,C\,m^2$.

4. Discussion

This EFGIB investigation has yielded a molecular electric quadrupole moment of $\Theta = (-1.033 \pm 0.027) \times 10^{-40}\,C\,m^2$ for O_2. Since the measurements were obtained at room temperature, the extraction of the quadrupole moment Θ from the measured $_mQ$ data via Eq. (6) has been achieved by assuming the b' contribution to be negligible, i.e. setting b' to zero.

Only one previous EFGIB determination of Θ for O_2 exists, undertaken at room temperature by Buckingham et al., and yielding $\Theta = (-1.33 \pm 0.33) \times 10^{-40}\,C\,m^2$ [26]. Here, the uncertainty is 25%, and the b' term has been assumed to be zero. Cohen and Birnbaum have obtained Θ for O_2 using the indirect approach of analyzing pressure-induced far-infrared spectra [27]. These results are dependent on the model used to describe the intermolecular interaction potential, and are generally not considered to be particularly reliable. For O_2 they obtained $\Theta = |1.1| \times 10^{-40}\,C\,m^2$, which is in reasonable agreement with our value.

The temperature-independent b'-term's contribution to the induced birefringence of small molecules has been found to range from around 3% for CO_2 [6] up to 10% for N_2 [11]. Clearly, this term typically makes a small but non-negligible contribution to the EFGIB, and so needs to be accounted for if a definitive quadrupole moment is to be extracted from the measured data. This can be achieved in one of two ways: either a full temperature-dependent experimental study can be undertaken, so that the temperature-independent and temperature-dependent contributions to $_mQ$ can be separated out; or the b' term can be calculated by *ab initio* quantum computational techniques, allowing for Θ to be accurately extracted from $_mQ$ using Eq. (6).

Table 2
A comparison of selected molecular electric quadrupole moments for O_2.

$10^{40}\Theta$ ($C\,m^2$)	Method	Reference
-1.033 ± 0.027	EFGIB (single temp., $b' = 0$)	This work
-1.33 ± 0.33	EFGIB (single temp., $b' = 0$)	[26]
$\|1.0\|$	Pressure-induced far IR spectrum	[28,29]
$\|1.1\|$	Pressure-induced far IR spectrum	[27]
-1.184	SCF computation	[30]
-1.218	CI-perturbation computation	[31]
-1.185	RAS computation	[32]
-1.020	CBS-CASSCF+1+2 computation	[33]
-1.140	MCSCF computation	[34]
-1.010	ACPF computation[a]	[1]

[a] This is considered to be the most reliable *ab initio* computation to date.

The measured $_mQ$ of O_2 is extraordinarily tiny, being some 28 times smaller than the CO_2 $_mQ$ at room temperature, and a consequence of this has been an inability to realize measurements of $_mQ$ for O_2 at higher temperatures using our current experimental arrangement. While a full temperature-dependent study of the Buckingham effect for O_2 is desirable, considerable experimental challenges will need to be overcome before this can be realized.

A tabulation of our quadrupole moment for O_2, together with selected values obtained by other researchers, is provided in Table 2. Here we see that earlier *ab initio* calculations of Θ have tended to yield larger absolute values than the most recent $\Theta = -1.010 \times 10^{-40}\,C\,m^2$ obtained by Bartolomei et al., which has been attributed to the lack of dynamic electron correlation in the previous calculations [1]. The *ab initio* calculations of Bartolomei et al. are performed at the multiconfigurational self-consistent field (MCSCF) level of theory, and include methods which account for dynamic electron correlation effects, such as the multireference averaged coupled pair functional (ACPF) theory. Their preferred value is 2.3% larger (less negative) than our experimental value, the agreement being quite good. It should be noted that Bartolomei et al. have not included vibrational corrections in their computed Θ, which could partially account for the small discrepancy between experiment and theory.

If theoreticians pursue *ab initio* computations of the b' term for this molecule, it will be interesting to see whether correction of our measured Θ brings the experimental and calculated quadrupole moments of O_2 into better agreement. The effect of inclusion of vibrational averaging in the *ab initio* computation of Θ itself would also be worth examining.

Acknowledgements

This work has been supported by the South African National Laser Centre (NLC). S.S.N. also gratefully acknowledges the award of a NITheP graduate bursary.

References

[1] M. Bartolomei, E. Carmona-Novillo, M.I. Hernández, J. Campos-Martínez, R. Harnández-Lamoneda, J. Comp. Chem. 32 (2011) 279.
[2] T. Helgaker, S. Coriani, P. Jørgensen, K. Kristensen, J. Olsen, K. Ruud, Chem. Rev. 112 (2012) 543.
[3] M. Lepers, B. Bussery-Honvault, O. Dulieu, J. Chem. Phys. 137 (2012) 234305.
[4] A.D. Buckingham, J. Chem. Phys. 30 (1959) 1580.
[5] A.D. Buckingham, R.L. Disch, Proc. R. Soc. A 273 (1963) 275.
[6] N. Chetty, V.W. Couling, Mol. Phys. 109 (2011) 655.
[7] N. Chetty, V.W. Couling, J. Chem. Phys. 134 (2011) 144307.
[8] N. Chetty, V.W. Couling, J. Chem. Phys. 134 (2011) 164307.
[9] A. Halkier, S. Coriani, P. Jørgensen, Chem. Phys. Lett. 294 (1998) 292.
[10] S. Coriani, C. Hättig, P. Jørgensen, A. Rizzo, K. Ruud, J. Chem. Phys. 109 (1998) 7176.
[11] G.L.D. Ritchie, J.N. Watson, R.I. Keir, Chem. Phys. Lett. 370 (2003) 376.
[12] J. Vrbancich, G.L.D. Ritchie, J. Chem. Soc., Faraday Trans. 2 (76) (1980) 648.
[13] A.D. Buckingham, H.C. Longuet-Higgins, Mol. Phys. 14 (1968) 63.
[14] A.D. Buckingham, M.J. Jamieson, Mol. Phys. 22 (1971) 117.
[15] A.D. Buckingham, M. Pariseau, Trans. Faraday Soc. 62 (1966) 1.
[16] J.H. Dymond, K.N. Marsh, R.C. Wilhoit, K.C. Wong, The Virial Coefficients of Pure Gases and Mixtures, Springer-Verlag, Berlin, 2002.
[17] K.-H. Hellwege, A.M. Hellwege (Eds.), Landolt-Börnstein, Zahlenwerte und Funktionen, Springer-Verlag, Berlin, 1962, Band II, Teil 8.
[18] J.W. Schmidt, M.R. Moldover, Int. J. Thermophys. 24 (2003) 375.
[19] E.F. May, M.R. Moldover, J.W. Schmidt, Phys. Rev. A 78 (2008) 032522.
[20] N.J. Bridge, A.D. Buckingham, Proc. Roy. Soc. Lond. Ser. A 295 (1966) 334.
[21] U. Hohm, Mol. Phys. 81 (1994) 157.
[22] F. Baas, K.D. van den Hout, Physica A 95 (1979) 597.
[23] M.P. Bogaard, A.D. Buckingham, R.K. Pierens, A.H. White, J. Chem. Faraday Trans. 1 (74) (1978) 3008.
[24] D. Jonsson, P. Norman, O. Vahtras, H. Ågren, A. Rizzo, J. Chem. Phys. 106 (1997) 8552.
[25] D.C. Baird, Experimentation: An Introduction to Measurement Theory and Design, Prentice Hall, Englewood Cliffs, NJ, 1964.
[26] A.D. Buckingham, R.L. Disch, D.A. Dunmur, J. Am. Chem. Soc. 90 (1968) 3104.
[27] E.R. Cohen, G. Birnbaum, J. Chem. Phys. 66 (1977) 2443.
[28] D.R. Bosomworth, H.P. Gush, Can. J. Phys. 43 (1965) 751.
[29] M. Evans, Mol. Phys. 29 (1975) 1345.
[30] J.H. van Lenthe, F.B. van Duijneveldt, J. Chem. Phys. 81 (1984) 3168.
[31] W. Rijks, M. van Heeringen, P.E.S. Wormer, J. Chem. Phys. 90 (1989) 6501.
[32] H. Hettema, P.E.S. Wormer, P. Jørgensen, H.J.A. Jensen, T. Helgaker, J. Chem. Phys. 100 (1994) 1297.
[33] D.B. Lawson, J.F. Harrison, J. Phys. Chem. A 101 (1997) 4781.
[34] B.F. Minaev, Spectrochim. Acta A 60 (2004) 1027.